Pre-print version accepted on 14/06/2016 Journal of Plankton Research

doi: 10.1093/plankt/fbw052

Nitrogen inputs influence on biomass and trophic structure of ocean plankton: a study using biomass and stable isotope size-spectra

Carmen Mompeán[1], Antonio Bode[1*], Mikel Latasa[3], Bieito Fernández-Castro[2], Beatriz Mouriño-Carballido[2] and Xabier Irigoien[4,5]

[1] Instituto Español de Oceanografía, Centro Oceanográfico de A Coruña, Apdo. 130, E15080 A Coruña, Spain

[2] Departamento de Ecología y Biología Animal, Universidad de Vigo, E36310 Vigo, Spain

[3] Instituto Español de Oceanografía, Centro Oceanográfico de Gijón/Xixón, Avda. Príncipe de Asturias 70bis, E33212 Gijón/Xixón, Spain

[4] AZTI, Arrantza eta Elikaigintzarako Institutu Teknologikoa, Herrera Kaia portualdea, 20110 Pasaia, Spain.

[5] Present address: King Abdullah University of Science and Technology [KAUST], Red Sea Research Center, Thuwal 23955-6900, Saudi Arabia

Keywords: stable isotopes, $\delta^{15}N$, plankton, ocean, food web, biomass, size spectrum

Running title: trophic structure of ocean plankton

***Corresponding author:** Antonio Bode (antonio.bode@co.ieo.es)

ABSTRACT

Large scale patterns in planktonic food web structure were studied by applying continuous size-scaled models of biomass and $\delta^{15}N$ to plankton samples, collected at 145 stations during the Malaspina-2010 Expedition across three ocean basins and including major biomes. Carbon biomass

and $\delta^{15}N$ were determined in size-fractionated samples (40 to 5000 μm) collected by vertical hauls (0-200 m). Biomass-normalized size-spectra were constructed to summarize food web structure and spatial patterns in spectral parameters were analyzed using geographically-weighted regression analysis. Except in the northwestern Atlantic, size-spectra showed low variability, reflecting a large homogeneity in nitrogen sources and food web structure for the central oceans. Estimated predator-to-prey mass ratios $<10^4$ and mean trophic transfer efficiency values between 16% (coastal biome) and >20% (Trades and Westerlies biomes) suggested that oceanic plankton food webs could support a larger number of trophic levels than current estimates based on high efficiency values. The largest changes in spectral parameters and nitrogen sources were related to inputs of atmospheric nitrogen, either from diazotrophic organisms or dust deposition. These results suggest geographic homogeneity in the net transfer of nitrogen up the food web.

INTRODUCTION

Ocean plankton is an essential contributor to the dynamics of the earth climate system. Phytoplankton drawdown of CO_2 is made at the expenses of nutrients as nitrogen, and the fate of the organic matter produced depends on the characteristics of the food web, that in turn are largely determined by the size of planktonic organisms (Legendre and Lefevre, 1995). The effects of warming and increasing stratification imply reductions in the input of nutrients from deep waters to the surface ocean and subsequent changes in primary production in large ocean areas (Behrenfeld *et al.*, 2006). Depending on the structure of the food web the climate effects can be amplified or modified as shown by both *in situ* (Richardson and Schoeman, 2004) and modeling studies (Chust *et al.*, 2014). Thus, determining the structure of the food web is essential for understanding the behavior of the ocean ecosystems under a changing climate.

Based on the dependency of most physiological processes on organism size, models relating organism abundance (or biomass) and individual size have been developed with the purpose of describing the continuous change of biomass across the whole food web (Platt and Denman, 1978; Blanco *et al.*, 1994). The so-called size-spectrum models have been used to synthesize the food web structure in comparative analysis of oceanic ecosystems (Rodriguez and Mullin, 1986; Piontkovski *et al.*, 2003; Quiñones *et al.*, 2003; San Martin *et al.*, 2006). Furthermore, they have been used to infer the maximum number of trophic levels that a particular ecosystem can support (Zhou, 2006; Basedow *et al.*, 2010). Their applicability has been questioned as their predictions generally require steady state conditions and uniformity in the size-dependent physiological rates (Poulin and Franks, 2010), but some of these limitations can be overcome by models (Ward et al., 2014) or the use of seasonal averages (Hunt et al.,2015).

Stable isotope analysis provides an important tool for elucidating trophic structure. For instance, enrichment in ^{15}N has been observed with increasing trophic position, thus allowing to infer trophic structure (e.g. Post, 2002). This enrichment can also be expected across plankton size classes, as pelagic food webs are strongly size-structured, the smallest organisms being generally primary producers and large organisms consumers of smaller prey (Platt and Denman, 1978). However, only a few field studies explored the implications of the variability in ^{15}N with plankton size (Fry and Quiñones, 1994; Rolff, 2000; Bode *et al.*, 2007; Jennings et al., 2008; Mompeán *et al.*, 2013). One of the main limitations was the difficulty in obtaining measurements over a large number of size classes representative of the different trophic levels. The adjustment of simple continuous functions was not always possible because of the frequent exceptions to the general increase of ^{15}N with the average size of the organisms sampled size. For instance, plankton of total length smaller than 200 µm tend to show lower variability in average ^{15}N content than plankton in larger size classes (Rolff, 2000; Bode *et al.*, 2007). This is due both to the high variability at short time scales in small size classes owing to fast turnover times, thus reflecting rapid changes in the N sources (e.g. Jennings et al., 2008), but also to the small changes in isotopic composition observed in microbial food webs (e.g. Gutierrez-Rodriguez et al., 2014). In addition, the presence of large or colonial plankton that feed on phytoplankton caused a decrease in ^{15}N at large sizes, while there is a lineal increase with plankton size when these large herbivores were not present (Fry and Quiñones, 1994; Hunt et al., 2015). Besides, because most studies used net sieves with a logarithmic increase in mesh size, the direct comparison of ^{15}N content with size did not allowed for the computation of significant linear functions in some of the samples, even when considering a relatively large range of sizes (e.g. Rolff, 2000). As for the biomass distributions, the use of logarithmic transformations and normalization of the variable of interest (^{15}N in this case) by the biomass of the organisms may lead to the construction of size-spectra that allow inferences on the trophic structure of plankton independently of the actual range of sizes measured. To our knowledge, this study represents the first application of biomass-normalized size spectra using stable isotopes.

Large regions of the open ocean are poorly sampled. Here, food webs are generally characterized by low nutrient concentrations, low biomass and dominance of microbial recycling of nutrients with some exceptions due to external nutrient supply (Longhurst, 2007). Studies analyzing the planktonic size structure at large oceanic scales are scarce (Piontkovstki *et al.*, 2003; Quiñones *et al.*, 2003; San Martín *et al.*, 2006) while there are no studies addressing the changes of stable nitrogen isotopes with plankton size at such scales. Meta-analyses of planktonic isotopic composition on plankton at large geographic scales have shown latitudinal patterns that were related to the sources and bioavailability of nutrients (Bowen, 2010; McMahon et al., 2013). In this study we use biomass

and ^{15}N size spectra to assess whether the type of dominant source of inorganic nutrients affects the trophic structure of plankton in the open ocean. The underlying hypothesis is that the trophic structure of plankton in the open ocean will be determined by the balance between nutrient inputs from deep or continental waters or from the atmosphere. Advective inputs can be expected to be of importance at relatively small spatial or temporal scales, as those related to mesoscale dynamics (Oschlies and Garçon, 1998), while most of the nutrients for the oligotrophic ocean are provided by transport across the pycnocline (Mouriño-Carballido *et al.*, 2011; Torres-Valdés *et al.*, 2009; Fernández-Castro et al. 2015). Atmospheric inputs include biological N_2 fixation (Capone *et al.*, 2005; Mulholland, 2007) and deposition of inorganic and organic nutrients, the latter noticeably enhanced by anthropogenic emissions (Duce *et al.*, 2008). Advection of deep nutrients is expected to lead to blooms of phytoplankton of relatively large size, high primary production and metazoan food webs, typical of most temperate and polar regions, with a strong seasonal variability (Longhurst, 2007). Most of the open ocean is expected to depend on non-seasonal, relatively small inputs of nutrients by diffusion, leading to phytoplankton of small size, low primary production and rapid remineralization of organic matter in microbial food webs. Atmospheric N fixation can be due to either large phytoplankton (as the colony-forming cyanobacteria *Trichodesmium*) or to microbial forms, but in all cases low primary production and high microbial remineralization is expected before effective transfer of the fixed N up the food web (Mulholland, 2007). Because of the dependence of N fixation on micronutrients, as Fe provided by dust deposition (Moore *et al.*, 2009), atmospheric inputs of nutrients may have also a clear seasonal component. In all cases, the trophic structure of the food web will depend on the net amount of nutrients transferred from the primary producers to the various types of consumers. This implies, by assuming a constant transfer efficiency between trophic levels (Zhou, 2006), that most of the oligotrophic open ocean would have shorter food webs than productive seasonal regions, as the biomass of pelagic predators depends on the amount of primary production (Chassot *et al.*, 2007). However, a larger number of trophic steps is expected in the oligotrophic ocean because the rapid recycling of organic matter in microbial food webs (Sommer et al., 2002).

The objective of this study is to investigate the relationships between plankton trophic structure and the source of N at large-scale spatial scales in the ocean. For this purpose we analyzed carbon biomass and the natural abundance of stable nitrogen isotopes in a large set of size-fractionated plankton samples from the research expedition Malaspina-2010 across three ocean basins.

METHODS

Plankton sampling and analysis

Plankton samples were collected during Malaspina-2010 expedition between December 2010 and July 2011 (Fig. 1). The expedition employed two oceanographic ships to make observations and collect water, seston and plankton samples across three major ocean basins (http://metamalaspina.imedea.uib-csic.es/geonetwork/srv/en/main.home). In this study plankton samples from 145 stations were considered. Samples were collected by vertical hauls of bongo-type nets (30 cm diameter, 40 µm mesh size and 50 cm diameter, and 200 µm mesh size) between 200 m depth and the surface during early morning hours. Plankton was size-fractionated using sieves of 200, 500, 1000, 2000 and 5000 µm, collected on pre-weighted glass-fiber filters and oven dried (60°C, 24 h) on board. Large gelatinous organisms were removed and analyzed separately (Molina-Ramirez et al., 2015). In addition, sample aliquots were preserved in formalin (4% final concentration) for later determination of the abundance of trichomes of the N-fixing cyanobacterium *Trichodesmium*. Counts were made using a semiautomatic image analysis flow-through system (FlowCam).

Biomass was later determined in the laboratory for each size fraction as carbon (C) and nitrogen content using an elemental analyzer (Carlo Erba CHNSO 1108). No acidification treatment to remove carbonates was applied prior to analysis of carbon, but molar C:N values (mean ± se = 4.8 ± 1.39, n = 145) were typical of planktonic organic matter (Søreide et al., 2007) and indicated that the possible overestimation of C due to inorganic carbon would be small. Natural abundance of stable nitrogen isotopes was determined using a mass spectrometer (Finnigan Mat Delta Plus) coupled to the elemental analyzer. Nitrogen stable isotope abundance were expressed as $\delta^{15}N$ (‰) relative to atmospheric nitrogen (Coplen, 2011). International Atomic Energy Agency (IAEA) USGS40 and L-alanine isotope standards were analyzed with the samples, along with internal acetanilide and sample standards. Precision (±se) of replicate determinations of standards and samples was <0.1‰ (n= 2 to 6) and <0.3‰ (n= 5 to 10), respectively. The analytical offset between certified and measured values was <0.1‰. All isotopic determinations were made in the Servicio de Análisis Instrumental of the Universidade da Coruña (Spain). Further details on the sampling and analysis can be found in Moreno-Ostos (Moreno-Ostos, 2012) and Mompeán *et al.* (Mompeán *et al.*, 2013).

Oceanographic conditions *in situ*

Hydrographic information was obtained from CTD-rosette casts at the same stations and chlorophyll-a (Chl*a*) was determined from acetonic extracts of phytoplankton collected at up to 8 discrete depths in the photic layer (>0.1% of surface photosynthetically active irradiance). Here Chl*a* values were integrated in the photic layer as a proxy for phytoplankton biomass. In addition, the vertical extent of phytoplankton was estimated by the depth of the chlorophyll maximum

(DCM). As nutrient concentrations and fluxes were not available for all the sampled stations (Fernández-Castro et al., 2015), several proxies for nutrient supply from deep waters were employed. First, the DCM itself, as it was negatively correlated with the flux of nitrate (Fig. 1S). Second, the stratification of the upper water column (Behrenfeld et al., 2006). estimated by the mixing layer depth (MLD), computed using a density difference criterion ($\Delta\delta$ = 0.125 kg m^{-3} with respect to surface values), and the mean squared Brunt-Väisälä frequency (N^2) values computed at 1 m intervals for the upper 200 m. Additional details on the sampling and on the analytical methods employed can be found in Moreno-Ostos (Moreno-Ostos, 2012).

Satellite observations

As the observed plankton properties (i.e. biomass, stable isotopes) at each station would be the consequence not only of local conditions but also of general oceanographic conditions prevailing over a certain amount of space and time, additional variables, estimated from satellite observations, were also considered. Annual averages of primary production for 2010 (PP, mg C m^{-2} d^{-1}) were generated by averaging monthly data for primary production downloaded from the Ocean Productivity website (http://www.science.oregonstate.edu/ocean.productivity/index.php) from the grid (0.17° x 0.17°) closest to each station position.

Dust deposition, as a proxy for atmospheric inputs of key nutrients for primary production (e.g. Fe or P), was also estimated from Aqua-MODIS Aerosol Optical Depth at 550 nm and Aerosol Small Mode Fraction data provided by the Giovanni online data system (NASA Goddard Earth Sciences). These data were retrieved from a grid of 1° resolution and centered at the closest location to each station and combined with wind speed derived from AVISO (http://las.aviso.oceanobs.com/las/getUI.do) to estimate the monthly average atmospheric dust column concentration (MDU, g m^{-2}) at each station (Kaufman *et al.*, 2005).

Creation of size spectra

Biomass and $\delta^{15}N$ values by size fractions of plankton were combined in the form of linear regressions with the median size of individuals in the corresponding size fraction. This median size was estimated as the geometric mean of the nominal size (length) of the sieves employed for each class, and further calculation of carbon biomass by using conversion factors (Rodriguez and Mullin, 1986). Due to the large variability in the values, a single regression including all stations sampled was not possible (Fig. 1S). Logarithmic transformations ($\log_2$) and normalization by the width of the interval of individual biomass were applied to obtain functions independent from size-class width (Blanco *et al.*, 1994, Zhou, 2006). The resulting biomass-normalized lines (obtained by least

squares regression) characterized the size distribution of biomass or $\delta^{15}N$ by two parameters: the intercept (C_a, $\delta^{15}N_a$), a proxy for the values in the first size class, and the slope (C_b, $\delta^{15}N_b$), indicative of the rate of change in the values with increasing individual size (Fig. 2). Individual values of spectral regression parameters for each station are provided in the Supplement (Table 1S). The normalization procedure can be reversed to obtain un-normalized values of the slope that can be further used to develop several descriptors of food web properties (Blanco et al., 1994). For instance, we computed the number of trophic levels (NTL) from C_b (Zhou, 2006), the predator-to-prey mass ratio (PPMR) from the slope *m* of the un-normalized $\delta^{15}N$ spectrum (Jennings *et al.*, 2001), and the trophic transfer efficiency (TTE) from PPMR (Barnes *et al.*, 2010). Where:

$$NTL = - (1+0.7) / (C_b\ 0.7)$$

by assuming a trophic efficiency (i.e. the ratio of production of predator to its prey) of 0.7 (Zhou, 2006),

$$PPMR = 2^{2.2/m}$$

by assuming a $\delta^{15}N$ enrichment between trophic levels of 2.2‰, appropriate for plankton, ammonotelic organisms which show lower $\delta^{15}N$ enrichment than consumers excreting urea (Vanderklift and Ponsard, 2003; Hunt et al., 2015), and:

$$TTE = PPMR^{-1.05+0.75}$$

by assuming a time averaged un-normalized biomass slope of -1.05 (Barnes et al., 2010; Hunt et al., 2015).

In addition, the trophic position of the largest plankton size class (TP_{2000}) was computed from their $\delta^{15}N$ values ($\delta^{15}N_{2000}$) as:

$$TP_{2000} = TP_{40} + \frac{\delta^{15}N_{2000} - \delta^{15}N_{40}}{2.2}$$

where TP_{40} is the trophic position of the 40-200 µm size class used as the reference baseline by assuming that it contained a mixture of phytoplankton and microzooplankton (TP_{40} = 1.5), and a constant $\delta^{15}N$ enrichment between adjacent trophic levels of 2.2‰ (Hunt et al., 2015).

Spatial analysis

Stations were first grouped by biomes (Longhurst, 2007) (Fig. 1) to investigate large scale differences in biomass and spectral parameters using ANOVA and Dunnett-C post-hoc tests.

Visualization and further analysis of trends at various spatial scales were made using the tools provided by the package Spatial Analysis in Macroecology (SAM V 4.0) which allowed mapping and computation of various spatial statistics from metrics descriptive of spatial autocorrelation to advanced spatial regression (Rangel *et al.*, 2010). Spatial autocorrelation of variables was analyzed by means of correlograms of the Moran's I coefficient computed for groups of samples (stations) of increasing spatial distance. The relationships between spectral parameters and environmental variables were investigated using principal components analysis (PCA) to determine the main correlations. Then, we selected the most representative environmental variables to construct regression models explanatory of each of the spectral parameters at each station using Geographically Weighted Regression (GWR). This method, specifically designed to deal with spatial autocorrelation and lack of stationarity (Rangel et al., 2010), was used to compute a series of local regressions, one for each station location, between the independent variable (i.e. spectral parameters) and the explanatory variables (i.e. selected environmental variables) taking into account the information from the surrounding stations weighted by a spatial function. In this case we used a moving spatial window with an adaptive Kernel of 15% of neighboring stations optimized using the Akaike's Information Criterion. The explanatory power of GWR (r^2) for each spectral parameter was in general higher than those of ordinary least squares, as measured by ANOVA tests (Rangel *et al.*, 2011).

RESULTS

Spatial distributions

Biomass and $\delta^{15}N$ showed an uneven distribution across the ocean as illustrated by the maps for the 40-200 μm size-class (Fig. 3). In contrast, the values for the parameters characterizing biomass and $\delta^{15}N$ spectra showed in general low variability, resulting in a relatively homogeneous distribution at large spatial scales (Fig. 4, Fig. 3S). An exception was the Subtropical North Atlantic region (cruise legs 7 and 8), mostly in the Westerlies biome. Here, the intercepts for both biomass and $\delta^{15}N$ spectra (C_a and $\delta^{15}N_a$) reached in general lower values than in other regions, while the slopes (C_b and $\delta^{15}N_b$) showed high variability. This latter pattern is a response to the low ^{15}N values measured in the 40-200 μm size-class (Fig. 3) in the subtropical regions thus producing an overall negative correlation with latitude ($r=-0.507$, $P<0.001$, $n=145$). The geographic and temporal distribution of samples also affected in complex ways to these distributions, as there were positive correlations between $\delta^{15}N_b$ and either latitude ($r=0.331$, $P<0.001$) or sampling date ($r=0.202$, $P<0.05$). When grouped by biomes, the differences were significant in the Westerlies (including the southern Australia region) for all parameters and variables, except for $\delta^{15}N_b$ (Table 1). Thus, the lower

biomass and $\delta^{15}N$ values at the base of the planktonic food web in the Westerlies biome ($C_{40\text{-}200}$ and $\delta^{15}N_{40\text{-}200}$) affected the food web structure represented by size spectra.

The trophic position of the largest plankton size-class sampled was significantly correlated with the slope of the $\delta^{15}N$ spectra (Fig. 4S) and reached values generally below 2, particularly for the samples in the coastal biome (Table 2). In contrast, estimates using the biomass spectra resulted in a maximum number of ca. 3 trophic levels. Mean values of PPMR were below 1000 and no significant differences were found between biomes, while mean TTE was 16% for the coastal biome and >20% for the Trades and Westerlies biomes (Table 2).

The distribution of annual primary production (Fig. 3S f) was also quite homogeneous across the sampled ocean regions, while variables indicative of different nutrient inputs, as the abundance of *Trichodesmium*, the depth of the chlorophyll maximum or the atmospheric dust deposition were more heterogeneously distributed (Fig. 5, Fig. 3S). *Trichodesmium* abundance was present in all regions but showed in general high values in the North Atlantic (legs 7 and 8). The chlorophyll maximum was deepest in the central regions of all ocean basins. The distribution of other variables as the depth of the mixing layer or the Brunt-Väisälä frequency (not shown) had also variability at intermediate and large spatial scales but otherwise they were significantly correlated with the depth of the chlorophyll maximum ($r = -0.355$, $P<0.01$, $n = 137$). Relatively high dust deposition was estimated in the North Pacific and in the North Atlantic, but in the latter there were large differences between the values corresponding to different cruise legs in this region. For instance, the largest dust deposition corresponded to the spring-summer leg and the lowest to the winter leg (Fig. 5c, Fig. 3S g).

Correlations of spectral and other variables

We found correlation between the intercepts of each spectrum type (biomass or $\delta^{15}N$) and the values measured at the smallest size class (40-200 μm), as expected. There was also a negative correlation between the slopes of biomass and $\delta^{15}N$ spectra. All these correlations can be characterized by the angle between vectors in the space of the two main components of the PCA, explaining 46.3% of total variance (Fig. 6). It should be highlighted the negative correlations between $\delta^{15}N_a$ and the depth of the chlorophyll maximum (DCM) and the abundance of *Trichodesmium*, and the positive correlations between C_a and chlorophyll and primary production. In turn, $\delta^{15}N_b$ showed positive correlation with mean dust deposition and DCM while C_b was negatively correlated with DCM. Interestingly, DCM can be considered a better index of nutrient inputs across the thermocline than the depth of the mixing layer (MLD), as it was positively

correlated with MLD and also with chlorophyll-*a*, primary production, biomass and $\delta^{15}N$ of the 40-200 μm size-class.

Geographically weighted regression models

From the global correlation and PCA results we selected the independent variables DCM (as an index of the vertical transport of nutrients across the thermocline), *Trichodesmium* abundance (as a proxy for atmospheric nitrogen fixation) and MDU (as a proxy for other atmospheric nitrogen inputs) to construct regression models explanatory of the spectral parameters (C_a, C_b, $\delta^{15}N_a$, $\delta^{15}N_b$) at local scale using GWR models (Table 3). Most GWR models were significant ($P<0.001$) and only the GWR model for C_b resulted non significant ($P=0.070$) and with less explanatory power than ordinary least squares (the latter with a relative decrease of 33.035 in the Akaike Information Criterion). The spatial autocorrelation of spectral variables and residuals indicated by Moran's I values (Fig. 7) showed that the spatial structure was better represented at all spatial scales in the case of $\delta^{15}N$ models, with lower residuals than models for biomass. The median values of the model parameters indicated that the distribution of the dependent variables was determined mainly by a constant value modulated by the coefficients of the independent variables (Table 3). *Trichodesmium* abundance and DCM had marginal influence in general (median values close to 0) but their range of values indicated some local influence. In contrast, median values for MDU coefficients ranked second after the constant values, suggesting that this variable was important for determining the shape of $\delta^{15}N$ spectra and the biomass at the base of the food web (C_a).

DISCUSSION

The results of this study showed that the size spectra of stable nitrogen isotopes added a new dimension to characterize the structure of planktonic food webs across the ocean. The parameters defining the size spectrum at each particular region were correlated with the main sources of nutrients for primary production, as the vertical transport across the thermocline and atmospheric inputs. Thus, the use of stable isotope spectra complement the information provided by biomass spectra, which were already established as an useful tool for describing and modeling the structure and function of pelagic ecosystems (Rodriguez and Mullin, 1986; Quiñones *et al.*, 2003; San Martin *et al.*, 2006; Zhou, 2006). The large number of observations collected across three ocean basins in our study suggests that the resulting relationships are of general application to all pelagic environments.

Isotope size-spectra in the central region of the ocean

316 The samples used in this study do not cover all possible oceanic conditions as most of the
317 observations were made in central areas of the ocean. Also, temporal variability (e.g. seasonality)
318 was not taken into account for most regions. However, three of the four ocean biomes were covered
319 (only the polar biome was not included in the study), and the range of primary production values
320 was representative of most of the open ocean, even including some data from the most productive
321 upwelling regions (e.g. Benguela). In addition, the observations across the subtropical North
322 Atlantic were made in two different seasons (winter-early spring and late spring-summer) thus
323 providing some hints for temporal variability, at least in this region. This is supported by the overall
324 correlations with the sampling date for either $\delta^{15}N_{40}$ or $\delta^{15}N_b$. In agreement with the low relative
325 importance of seasonality for plankton in the tropical and subtropical ocean (Longhurst, 2007), we
326 found small differences in size-spectra in this region, even when there were large differences in dust
327 inputs between transects made in different seasons (Fig. 5 c, Fig. 3S g). Short term variability (e.g.
328 those caused by nycthemeral migrations of plankton between deep and surface layers) is likely to
329 have a small effect on our results as the sampling was conducted approximately at the same period
330 of the day through all cruises.

331 The range of individual sizes considered could also influence the estimation of the parameters of the
332 spectra (Blanco et al., 1994). Besides, a large fraction of the primary production in the central
333 regions of the ocean is due to phytoplankton cells much smaller than the sizes considered in our
334 samples (Marañón, 2009). Although we employed only 5 discrete size-classes to construct the
335 spectra, they included organisms ranging from 10 ng C to 0.5 mg C individual weight (i.e. four
336 orders of magnitude). An inspection of some of the samples collected indicated a good
337 representation of phytoplankton (including diatoms, dinoflagellates, phytoflagellates and
338 cyanobacteria), and zooplankton filter-feeders and predators (Mompeán *et al.*, 2013). This wide
339 range of organisms, along with the robust character of biomass-normalized size-spectra that allows
340 for estimations of properties of the plankton community outside the actual range of fitted sizes
341 (Blanco *et al.*, 1994), supports the validity of our estimations for the plankton food web. In the case
342 of $\delta^{15}N$, previous studies showed that the spectra are continuous across the whole pelagic food web
343 (Jennings *et al.*, 2001; Bode *et al.*, 2007; Barnes et al., 2010; Hunt et al., 2015).

344 **Size-spectra and nutrient sources**

345 When considering biome scales, our results show large homogeneity in the parameters defining the
346 size spectra. Only the Westerlies biomes resulted with lower values of intercept and slope in the
347 biomass spectra, and also lower intercept values of the $\delta^{15}N$ spectra, than those computed for the
348 Trades and Coastal biomes. Such homogeneity in the size structure of the open ocean plankton can

be interpreted in terms of the main controls of the productivity. For most ocean regions, primary production is controlled by the availability of nutrients in the photic layer, and the main inputs depend on eddy diffusion through the pycnocline (Fernández-Castro et al., 2015) or advection of subsurface waters (Longhurst, 2007). These are likely the main fertilization mechanisms for the Trades and Coastal biomes, including productive upwelling in equatorial and coastal waters, while most of the subtropical oceans are occupied by oligotrophic gyres with reduced nutrient inputs and productivity (Behrenfeld *et al.*, 2006). Nevertheless, various mechanisms can provide local nutrient inputs, as mesoscale turbulence (Oschlies and Garçon, 1998), lateral transport from productive regions (Torres-Valdés *et al.*, 2009), atmospheric deposition (Duce *et al.*, 2008) and biological fixation of atmospheric nitrogen (Capone *et al.*, 2005). Notably, the subtropical North Atlantic is a region within the Westerlies biome where the fixation of nitrogen by diazotrophic plankton is favored by the deposition of Fe and phosphorus in dust particles (Capone *et al.,* 2005; Moore *et al.,* 2009; Fernández *et al.,* 2010). Notwithstanding the relative small fixation rates recorded in tropical and subtropical waters of the South Atlantic, they also contributed to a large fraction of total nitrogen inputs when compared to those from eddy diffusion (Mouriño-Carballido *et al.,* 2011). Only in the vicinity of upwelling areas the contribution of deep water nitrogen produced a traceable $\delta^{15}N$ signal in plankton (e.g. Fernández et al., 2010; Hauss et al., 2013; Mompeán et al., 2013) as observed in the increase of $\delta^{15}N_{40}$ from east to west in legs 7 and 8 (Fig. 3).

Our results show how the importance of these fertilization mechanisms translates into a significant correlation between indices of different nutrient sources and plankton biomass structure, the latter represented in this study by the parameters of the size spectra. Nutrient inputs from subsurface waters are indicated by the DCM, the layer where phytoplankton biomass accumulates because growth is maximized by a compromise between light levels (from above) and nutrient inputs (from below). The DCM, generally deeper when vertical advection/diffusion is low (e.g. at the centre of oligotrophic gyres) and shallower when is high (e.g. near upwelling areas), also could be seasonally affected. Previous studies have revealed that DCM is a better proxy for productivity than instantaneous nutrient concentrations in the surface layer (Mouriño *et al.*, 2004), and estimations of the vertical flux of nitrate during the Malaspina-2010 expedition (Fernández-Castro et al., 2015) were significantly correlated with the DCM (Fig. 1S). In the case of atmospheric inputs, biological nitrogen fixation is generally associated to the abundance of the colony-forming *Trichodesmium*, although unicellular diazotrophs may be also important, as found in most of the studied stations across the North Atlantic (Benavides *et al.*, 2016). Dust deposition favors nitrogen fixation, as it provides the necessary additional micronutrients (Moore *et al.,* 2009; Fernández *et al.,* 2010), but it also introduces significant nitrogen and phosphorus amounts (Morin *et al.,* 2009). Thus, the main

nutrient inputs can be used to model the biomass at the base of the food web, represented in our model by C_a.

Size-spectra and trophic structure

To our knowledge, this study represents the first application of biomass-normalized size spectra using stable isotopes. The increase in $\delta^{15}N$ with organism size is a general rule in pelagic food webs (Jennings *et al.,* 2001; Bode *et al.* 2007; Jennings *et al.* 2008; Barnes *et al.,* 2010; Hunt *et al.,* 2015). However previous studies of $\delta^{15}N$ in different size classes of plankton failed to demonstrate a regular increase in $\delta^{15}N$ with size, as there were many exceptions both at large and small organism sizes (Fry and Quiñones, 1994; Rolff, 2000, Bode *et al.,* 2007; Landrum *et al.,* 2011, Mompeán *et al.,* 2013). The planktonic exception can be attributed to the presence of large herbivores (as the colony-forming salps) but also to the different turnover times of biomass in organisms of different size (Jennings *et al.*, 2008). Besides, there are evidences of low or null enrichment in $\delta^{15}N$ within the microbial food web (Gutierrez-Rodriguez *et al.*, 2014). The normalization procedure applied in this study overcomes the lack of a regular increase in each local spectrum computed with raw values, as in previous studies. The biomass-normalized spectrum allows for a synthetic representation of the continuous distribution of the variable of interest across organism sizes by using only two parameters (Zhou, 2006). Besides, the reversal in the normalization (Blanco *et al.*, 1994) facilitates the determination of the values of the un-normalized slopes employed in estimations of PPMR and TTE (Barnes *et al.*, 2010). Such un-normalized slopes cannot be obtained in a larger number of cases using raw values (e.g. Fig. 2S). In this study, changes in the intercept of the $\delta^{15}N$ spectrum were related to the dominant source of nitrogen for primary producers, while changes in the slope were indicative of the overall isotopic enrichment along the food web.

Low intercepts are thus expected in areas with significant atmospheric inputs, either by diazotrophy or by inputs of anthropogenic nitrogen, as these sources have $\delta^{15}N$ values near zero (Morin *et al.,* 2009). This was the case of our observations in the Westerlies biome that had lower $\delta^{15}N_a$ than the Trades and Coastal biomes (Table 1), in agreement with the large importance of atmospheric nitrogen fixation in the former. However, we did not find significant differences in $\delta^{15}N_b$ between biomes and the detailed distribution of this parameter was very homogeneous across the ocean (Fig. 4d). This suggests that the transfer of nitrogen up the plankton food web proceeds, in general, at similar rates in all ocean regions. The exception was found in the two legs crossing the subtropical N Atlantic, where a large variability in $\delta^{15}N$ spectra was found in coincidence with relatively high amounts of *Trichodesmium* and other diazotrophs (Benavides *et al.*, 2016).

The relative homogeneity in the structure of oceanic plankton food webs suggested by $\delta^{15}N_b$ is supported by the low variability also observed in NTL, the latter independently estimated from C_b (Table 2). On average, NTL indicated that the oceanic plankton food webs analyzed had less than 3 trophic levels, with maximum values in the Coastal and Trades biomes. These values were ca. one trophic level higher than the estimations of the trophic position for the largest plankton size class using $\delta^{15}N$. The difference would suggest that these planktonic food webs would support only one additional consumer level predating upon the largest size class analyzed. Some of consumers may well be the cnidaria and ctenophora removed from the largest size fraction of our samples, with estimated TP between 2.6 and 2.9 (Molina-Ramirez et al., 2015). The trophic position of large plankton and the PPMR values obtained in our study are indicative of feeding on small plankton by most consumers. This is expected in oligotrophic waters dominated by picophytoplankton, (Hunt et al., 2015), thus suggesting a common trophic structure related to the nutrient inputs. The resulting TTE values were in the range observed for pelagic (Hunt et al., 2015) but also benthic ecosystems (Jennings et al., 2001) indicating a relatively high efficiency in the transfer of energy through the food web. However, these values were lower than the average estimated of 70% for pelagic food webs (Zhou, 2006). For instance, using a global TTE average of 21% would increase the NTL to 6.4, thus suggesting that the use of biomass spectra corrected by a TTE estimate from $\delta^{15}N$ would take into account the larger number of trophic steps expected in oligotrophic waters (Sommer et al., 2002).

The low variability observed in $\delta^{15}N$ slopes suggests that the overall trophic structure is similar across different planktonic communities, even when there are large variations in the nutrient sources and in the transmission of the energy through the food web. Organisms included in our spectra covered four orders of magnitude in individual size, implying a large difference in growth rates and biomass turnover times, and thus larger variability in $\delta^{15}N$ composition of the small plankton versus large plankton (Jennings *et al.*, 2008). Such differences would explain the reported delays in the transmission of the $\delta^{15}N$ signal from the N source (e.g. atmospheric N) to zooplankton predators (Rolff, 2000; Mompeán *et al.*, 2013). The normalization procedure applied in our study overcomes the time-lags and local variability of $\delta^{15}N$ and, as normalized biomass spectra, provides a better tool to compare different communities than un-normalized spectra. Similarity in $\delta^{15}N$ spectrum slopes and trophic structure across plankton communities can be expected if the underlying physiological processes are similar. Even when the nutrient (nitrogen) sources are different, the transmission up the food web is made by similar biochemical reactions for all planktonic communities. In the case of tropical and subtropical communities living in oligotrophic waters, recycling of dissolved organic matter through microbial communities is an important mechanism for transmission of nitrogen to

upper trophic levels (Mulholland, 2007). The homogeneity in trophic structure across pelagic ecosystems was already suggested by the first studies of biomass and abundance size spectra (Platt and Denman, 1978) and confirmed by subsequent studies including upper trophic levels (Hunt et al., 2015). Now, the application of biomass-normalized $\delta^{15}N$ spectra to whole food webs, including fish and upper consumers, can be used to analyze their variability by considering nitrogen exchanges.

CONCLUSIONS

Biomass and $\delta^{15}N$ size-spectra of plankton showed in general low variability, reflecting a large homogeneity in nitrogen sources and food web structure for the central oceans. The largest changes in spectral parameters and nitrogen sources were observed in the northwestern Atlantic and were related to inputs of atmospheric nitrogen, either from diazotrophic organisms or dust deposition. Mean predator-to-prey mass ratios between 4 and. $3 \cdot 10^3$ were estimated for all biomes, while mean trophic transfer efficiency values varied between 16% (coastal biome) and >20% (Trades and Westerlies biomes), thus suggesting that current estimates of the number of trophic levels based on a high average community efficiency may be too low, at least for most of the oligotrophic ocean. Both $\delta^{15}N$ and biomass size-spectra suggest geographic homogeneity in the net transfer of nitrogen up the food web.

ACKNOWLEDGEMENTS

We are grateful to all participants in the cruise legs for their collaboration in plankton sampling, to A.F. Lamas (IEO) for preparing samples for stable isotope analysis, to P. Chouciño and A. Fernández (UVigo) for assistance with the computation of dust deposition, to J. Lorenzo, J. Varela and M. Varela (IEO) for *Trichodesmium* counts, and to M. Estrada for useful comments to a first version of manuscript.

FUNDING

This research was supported in part by project Malaspina-2010 (CSD2008-00077) funded by program CONSOLIDER-INGENIO 2010 of the Ministerio de Ciencia e Innovación (Spain), project EURO-BASIN (FP7-ENV-2010 264933) of the EU, and by funds of the Instituto Español de Oceanografia (IEO). C.M. was supported by a PFPI grant of IEO. B. Fernández-Castro was supported by a FPU grant from the Spanish government (AP2010-5594).

DATA ARCHIVING

The biomass and stable isotope data used in this paper was deposited in the Malaspina-2010 repository and can be accessed through the following links:

http://metamalaspina.imedea.uib-csic.es:80/geonetwork?uuid=91b1175d-894c-4e48-980f-9cc325dcd79e

http://metamalaspina.imedea.uib-csic.es:80/geonetwork?uuid=4f79814e-ebab-4e0f-aea9-25c88bacd25a

Data from leg 8 are also available at the PANGAEA repository:

https://doi.pangaea.de/10.1594/PANGAEA.816451

490 **REFERENCES**

491 Barnes, C., Maxwell, D., Reuman, D. C. and Jennings, S. (2010) Global patterns in predator-prey
492 size relationships reveal size dependency of trophic transfer efficiency. *Ecology*, **91**, 222-232.
493 Basedow, S.L., Tande, K.S. and Zhou, M. (2010) Biovolume spectrum theories applied: spatial
494 patterns of trophic levels within a mesozooplankton community at the polar front. *J. Plankton*
495 *Res.*, **32**, 1105-1119.
496 Behrenfeld, M. J., O'Malley, R. T., Siegel, D. A., McClain, C. L., Sarmiento, J. L., Feldman, G. C.,
497 Milligan, A. J., Falkowski, P. G.. et al. (2006) Climate-driven trends in contemporary ocean
498 productivity. *Nature*, **444**, 752-755.
499 Benavides, M., Moisander, P. H., Daley, M. C., Bode, A. and Arístegui, J. (2016) Longitudinal
500 variability of diazotroph abundances in the subtropical North Atlantic Ocean. *J. Plankton Res.*,
501 **38**, 662-672.
502 Blanco, J. M., Echevarria, F. and Garcia, C. M. (1994) Dealing with size spectra: Some conceptual
503 and mathematical problems. *Sci. Mar.*, **58**, 17-29.
504 Bode, A., Alvarez-Ossorio, M. T., Cunha, M. E., Garrido, S., Peleteiro, J. B., Porteiro, C., Valdés,
505 L. and Varela, M. (2007) Stable nitrogen isotope studies of the pelagic food web on the Atlantic
506 shelf of the Iberian Peninsula. *Prog. Oceanogr.*, **74**, 115-131.
507 Bowen, G. (2010) Isoscapes: Spatial pattern in isotopic biogeochemistry. *Annu. Rev. Earth Planet.*
508 *Sci.*, **38**, 161-187.
509 Capone, D.G., Burns, J.A., Montoya, J.P., Subramaniam, A., Mahaffey, C., Gunderson, T.,
510 Michaels, A.F. and Carpenter, E.J. (2005) Nitrogen fixation by *Trichodesmium* spp.: An
511 important source of new nitrogen to the tropical and subtropical North Atlantic Ocean. *Global*
512 *Biogeochem Cycles*, **19**, doi:10.1029/2004GB002331.
513 Chassot, E., Mélin, F., Le Pape, O. and Gascuel, D. (2007) Bottom-up control regulates fisheries
514 production at the scale of eco-regions in European seas. *Mar. Ecol. Prog. Ser.*, **343**, 45-55.
515 Chust, G., Allen, J. I., Bopp, L., Schrum, C., Holt, J., Tsiaras, K., Zavatarelli, M., Chifflet, M., et al.
516 (2014) Biomass changes and trophic amplification of plankton in a warmer ocean. *GCB*
517 *Bioenergy*, doi: 10.1111/gcb.12562.
518
519 Coplen, T. B. (2011) Guidelines and recommended terms for expression of stable isotope-ratio and
520 gas-ratio measurement results. *Rapid Commun. Mass Spectrom.*, **25**, 2538-2560.
521 Duce, R. A., Laroche, J., Altieri, K., Arrigo, K. R., Baker, A. R., Capone, D. G., Cornell, S.,
522 Dentener, F. et al. (2008) Impacts of atmospheric anthropogenic nitrogen on the open ocean.
523 *Science*, **320**, 893-897.

524 Fernández, A., Mouriño-Carballido, B., Bode, A., Varela, M. and Marañón, E. (2010) Latitudinal
525 distribution of *Trichodesmium* spp. and N_2 fixation in the Atlantic Ocean. *Biogeosci.*, **7**, 3167-
526 3176.
527 Fernández-Castro, B., Mouriño-Carballido, B., Marañón, E., Chouciño, P., Gago, J., Ramírez, T.,
528 Vidal, M., Bode, A. et al. (2015) Importance of salt fingering for new nitrogen supply in the
529 oligotrophic ocean. *Nat. Geosci.*, **6**, doi:10.1038/ncomms9002.
530 Fry, B. and Quiñones, R.B. (1994) Biomass spectra and stable isotope indicators of trophic level in
531 zooplankton of the northwest Atlantic. *Mar. Ecol. Prog. Ser.*, **112**, 201-204.
532 Gutiérrez-Rodríguez, A., Décima, M., Popp, B. N. and Landry, M. R. (2014) Isotopic invisibility of
533 protozoan trophic steps in marine food webs. *Limnol. Oceanogr.*, **59**, 1590-1598.
534 Hauss, H., Franz, J. M. S., Hansen, T., Struck, U. and Sommer, U. (2013) Relative inputs of
535 upwelled and atmospheric nitrogen to the eastern tropical North Atlantic food web: Spatial
536 distribution of $\delta^{15}N$ in mesozooplankton and relation to dissolved nutrient dynamics. *Deep-Sea*
537 *Res*., **75**, 135-145.
538 Hunt, B.P.V., Allain, V., Menkes, C., Lorrain, A., Graham, B., Rodier, M., Pagano, M. and Carlotti,
539 F. (2015) A coupled stable isotope-size spectrum approach to understanding pelagic food-web
540 dynamics: A case study from the southwest sub-tropical Pacific. *Deep Sea Res. II*, **113**, 208-224.
541 Jennings, S., Maxwell, T.A.D., Schratzberger, M. and Milligan, S.P. (2008) Body-size dependent
542 temporal variations in nitrogen stable isotope ratios in food webs. *Mar. Ecol. Prog. Ser.* **370**,
543 199-206.
544 Jennings, S., Pinnegar, J. K., Polunin, N. V. C. and Boon, T. W. (2001) Weak cross-species
545 relationships between body size and trophic level belie powerful size-based trophic structuring in
546 fish communities. *J. Anim. Ecol.*, **70**, 934-944.
547 Kaufman, Y.J., Koren, I., Remer, L.A., Tanré, D., Ginoux, P. and Fan, S. (2005) Dust transport and
548 deposition observed from the Terra-Moderate Resolution Imaging Spectroradiometer (MODIS)
549 spacecraft over the Atlantic Ocean. *J. Geophys. Res.*, **110**, doi:10.1029/2003JD004436.
550 Landrum, J.P., Altabet, M.A. and Montoya, J.P. (2011) Basin-scale distributions of stable nitrogen
551 isotopes in the subtropical North Atlantic Ocean: Contribution of diazotroph nitrogen to
552 particulate organic matter and mesozooplankton. *Deep Sea Res.*, **58**, 615-625.
553 Legendre, L. and Le Fèvre, J. (1995) Microbial food webs and the export of biogenic carbon in
554 oceans. *Aquat. Microb. Ecol.*, **9**, 69-77.
555 Longhurst, A.R. (2007) *Ecological geography of the sea*. 2nd ed. Elsevier, Amsterdam
556 Marañón, E. (2009) Phytoplankton size structure. In: J. H. Steele, K. K. Turekian and S. A. Thorpe
557 (eds) *Encyclopedia of ocean sciences*. 2nd. ed. Academic Press, Oxford, pp. 4249-4256.

McMahon, K. W., Hamady, L. L. and Thorrold, S. R. (2013) Ocean ecogeochemistry: A review. Oceanogr. *Mar. Biol. Annu. Rev.* , **51**, 327-374.

Molina-Ramírez, A., Cáceres, C., Romero-Romero, S., Bueno, J., González-Gordillo, J. I., Irigoien, X., Sostres, J., Bode, A. et al. (2015) Functional differences in the allometry of the water, carbon and nitrogen content of gelatinous organisms. *J. Plankton Res.*, **37**, 989-1000.

Mompeán, C., Bode, A., Benítez-Barrios, V.M., Domínguez-Yanes, J.F., Escánez, J. and Fraile-Nuez, E. (2013) Spatial patterns of plankton biomass and stable isotopes reflect the influence of the nitrogen-fixer *Trichodesmium* along the subtropical North Atlantic. *J. Plankton Res.*, **35**, 513-525.

Moore, C. M., Mills, M. M., Achterberg, E. P., Geider, R. J., Laroche, J., Lucas, M. I., McDonagh, E. L., Pan, X. et al. (2009) Large-scale distribution of Atlantic nitrogen fixation controlled by iron availability. *Nat. Geosci.*, **2**, 867-871.

Moreno-Ostos, E. (ed.) (2012) *Expedición de circunnavegación Malaspina 2010. Cambio global y exploración de la biodiversidad del océano. Libro blanco de métodos y técnicas de trabajo oceanográfico.* Consejo Superior de Investigaciones Científicas (CSIC), Madrid.

Morin, S., Savarino, J., Frey, M.M., Domine, F., Jacobi, H.W., Kaleschke, L. and Martins, J.M.F. (2009) Comprehensive isotopic composition of atmospheric nitrate in the Atlantic Ocean boundary layer from 65°S to 79° N. *J. Geophys. Res. (D Atmos.)*, **114**, doi:10.1029/2008JD010696.

Mouriño, B., Fernández, E. and Alves, M. (2004) Thermohaline structure, ageostrophic vertical velocity fields and phytoplankton distribution and production in the northeast Atlantic subtropical front. *J. Geophys. Res.*, **109**, doi:10.1029/2003JC001990.

Mouriño-Carballido, B., Graña, R., Fernández, A., Bode, A., Varela, M., Domínguez, J.F., Escánez, J., De Armas, D. et al. (2011) Importance of N_2 fixation vs. nitrate eddy diffusion along a latitudinal transect in the Atlantic Ocean. *Limnol. Oceanogr.*, **56**, 999-1007.

Mulholland, M.R. (2007) The fate of nitrogen fixed by diazotrophs in the ocean. *Biogeosci.*, **4**, 37-51.

Oschlies, A. and Garçon, V. (1998) Eddy-induced enhancement of primary production in a model of the North Atlantic Ocean. *Nature*, **394**, 266-269.

Piontkovski, S. A., Landry, M. R., Finenko, Z. Z., Kovalev, A. V., Williams, R., Gallienne, C. P., Mishonov, A. V., Skryabin, V. A. et al. (2003) Plankton communities of the South Atlantic anticyclonic gyre. *Oceanol. Acta*, **26**, 255-268.

Platt, T. and Denman, K. (1978) The structure of pelagic marine ecosystems. *Rapp. P.-v. Réun. Cons. int. Explor. Mer*, **173**, 60-65.

592 Post, D. M. (2002) Using stable isotopes to estimate trophic position: Models, methods, and
593 assumptions. *Ecology*, **83**, 703-718.
594 Poulin, F.J. and Franks, P.J.S. (2010) Size-structured planktonic ecosystems: constraints, controls
595 and assembly instructions. *J. Plankton Res.*, **32**, 1121-1130.
596 Quiñones, R., Platt, T. and Rodriguez, J. (2003) Patterns of biomass-size spectra from oligotrophic
597 waters of the Northwest Atlantic. *Prog. Oceanogr.*, **57**, 405-427.
598 Rangel, T.F.L.V.B., Diniz-Filho, J.A.F. and Bini, L.M. (2010) SAM: a comprehensive application
599 for Spatial Analysis in Macroecology. *Ecography* **33**, 46-50
600 Rangel, T.F.L.V.B., Field, R. and Diniz-Filho, J.A.F. (2011) *SAM tutorial*. International
601 Biogeographic Society Meeting, Crete.
602 Richardson, A. J. and Schoeman, D. S. (2004) Climate impact on plankton ecosystems in the
603 Northeast Atlantic. *Science*, **305**, 1609-1612.
604 Rodriguez, J. and Mullin, M. M. (1986) Relation between biomass and body weight of plankton in a
605 steady state oceanic ecosystem. *Limnol. Oceanogr.*, **31**, 361-370.
606 Rolff, C. (2000) Seasonal variation in $\delta^{13}C$ and $\delta^{15}N$ of size-fractionated plankton at a coastal
607 station in the northern Baltic proper. *Mar. Ecol. Prog. Ser.,* **203**, 47-65.
608 San Martin, E., Irigoien, X., Harris, R.P., Lopez-Urrutia, A., Zubkov, M.V. and Heywood, J.L.
609 (2006) Variation in the transfer of energy in marine plankton along a productivity gradient in the
610 Atlantic Ocean. *Limnol. Oceanogr.*, **51**, 2084-2091.
611 Sommer, U., Stibor, H., Katechakis, A., Sommer, F. and Hansen, T. (2002) Pelagic food web
612 configurations at different levels of nutrient richness and their implications for the ratio fish
613 production:primary production. *Hydrobiologia*, **484**, 11-20.
614 Søreide, J. E., Tamelander, T., Hop, H., Hobson, K. A. and Johansen, I. (2007) Sample preparation
615 effects on stable C and N isotope values: A comparison of methods in arctic marine food web
616 studies. *Mar. Ecol. Prog. Ser.*, **328**, 17-28.
617 Torres-Valdes, S,, Roussenov, V.M., Sanders, R., Reynolds, S., Pan, X., Mather R., Landolfi, A.,
618 Wolff, G.A. et al. (2009) Distribution of dissolved organic nutrients and their effect on export
619 production over the Atlantic Ocean. *Glob. Biogeochem. Cycles*, **23**, doi:10.1029/2008GB003389.
620 Vanderklift, M. A. and Ponsard, S. (2003) Sources of variation in consumer-diet $\delta^{15}N$enrichment: A
621 meta-analysis. *Oecologia*, **136**, 169-182.
622 Ward, B. A., Dutkiewicz, S. and Follows, M. J. (2014) Modelling spatial and temporal patterns in
623 size-structured marine plankton communities: Top-down and bottom-up controls. *J. Plankton*
624 *Res.*, **36**, 31-47.
625 Zhou, M. (2006) What determines the slope of a plankton biomass spectrum? *J. Plankton Res.*, **28**,
626 437-448.

627

628 **Table and Figure legends:**

629 Table 1. Mean±se values of the parameters of the size spectra for biomass (C_a: intercept; C_b: slope)
630 and $\delta^{15}N$ ($\delta^{15}N_a$: intercept; $\delta^{15}N_b$: slope) and of carbon biomass ($C_{40\text{-}200}$, mg C m^{-3}) and $\delta^{15}N$
631 ($\delta^{15}N_{40\text{-}200}$, ‰) for the 40-200 µm size class in the three biomass sampled. Means not significantly
632 different are marked in the same group (ANOVA and Dunnett-C test, $P<0.05$). n: number of data.

633 Table 2. Mean±se values of the trophic position of the 2000-5000 µm size-class (TP_{2000}) and food
634 web parameters derived from size spectra in the three biomass sampled. NTL: number of trophic
635 levels (Zhou, 2006); PPMR: predator-to-prey mass rtio (Jennings et al., 2001); TTE: trophic transfer
636 efficiency, as % (Barnes et al., 2010). Means not significantly different are marked in the same
637 group (ANOVA and Dunnett-C test, $P<0.05$). n: number of data.

638 Table 3. Median, minimum (min) and maximum (max) values of GWR coefficients for spectral
639 parameters (C_a, $\delta^{15}N_a$ and $\delta^{15}N_b$) estimated from logarithmic *Trichodesmium* abundance (Tricho,
640 log trichomes m^{-3}), depth of chlorophyll maximum (DCM, m) and mean monthly dust deposition (g
641 m^{-2} $month^{-1}$). All models were fit with $P<0.05$ and include a constant term. Values from models for
642 C_b were not shown as GWR was not significant for this variable.

643 Table 1S. Parameters of the biomass-normalized biomass and $\delta^{15}N$ size-spectra determined for
644 plankton in the 0-200 m layer of stations of the Malaspina-2010 expedition. Lines in the form $Y = a$
645 $+ b \log_2(w)/\Delta w$ were fitted by least squares. w: mean individual size (µg C) of organisms in each
646 size-class; Δw: range of w for each size interval; r: correlation coefficient, se: standard error of the
647 regression. All parameters were significant ($P<0.05$).

648 Figure 1. Position of stations sampled during the Malaspina-2010 expedition for determination of
649 size-fractionated plankton biomass and natural abundance of stable nitrogen isotopes. The colors
650 indicate the biomes (black: Coastal, grey: Westerlies, white: Trades) according to Longhurst (2007).
651 The arrows and numbers indicate the different cruise legs and track direction.

652 Figure 2. Examples of size spectra for plankton samples collected at two stations of leg 8 of the
653 Malaspina-2010 expedition. a) un-normalized spectra for biomass (C, mg m^{-3}), b) un-normalized
654 spectra for $\delta^{15}N$ (‰), c) $\delta^{15}N$ biomass-normalized spectra. Mean biomass of the size class ($\log_2(w)$)
655 in µg C.

656 Figure 3. Distribution of plankton biomass (a, C_{40}, mg C m^{-3}) and $\delta^{15}N$ (b, $\delta^{15}N_{40}$ ‰) in the 40-200
657 µm size fraction for stations sampled during the Malaspina-2010 expedition. The vertical dashed

lines and numbers indicate the different cruise legs. The horizontal dashed line in b) indicates $\delta^{15}N=0$. Note the inversion of values in the horizontal axis for leg 8.

Figure 4. Distribution of parameters of biomass (a, b) and $\delta^{15}N$ (c, d) plankton size spectra computed for stations sampled during the Malaspina-2010 expedition. a), b): intercept of biomass (C_a) and $\delta^{15}N$ ($\delta^{15}N_a$) spectra, respectively. c), d): slope of biomass (C_b) and $\delta^{15}N$ ($\delta^{15}N_b$) spectra, respectively. Cruise legs indicated as in Fig. 3.

Figure 5. Distribution of *Trichodesmium* abundance (a, Tricho, log (trichomes+1) m^{-3}), depth of the chlorophyll maximum (b, DCM, m) and mean dust deposition (c, MDU, g m^{-2}) measured or estimated for stations sampled during the Malaspina-2010 expedition.

Figure 6. Vectors of variables projected in the space of the two main components of the PCA, . factors 1 and 2 accounting for 39% and 18% of total variance, respectively. C_a and C_b: intercept and slope of the biomass spectra, respectively; $\delta^{15}N_a$ and $\delta^{15}N_b$: intercept and slope of the $\delta^{15}N$ spectra, respectively; PP: primary production; Tricho: *Trichodesmium* abundance; MDU: mean dust deposition; MLD: mixed layer depth; DCM: depth of the chlorophyll maximum; C_{40} and $\delta^{15}N_{40}$: biomass and $\delta^{15}N$ of the 40-200 μm size-class, respectively; Chl*a*: chlorophyll concentration; N^2_m: mean squared Brunt-Väisälä frequency.

Figure 7. Spatial autocorrelation (Moran's I) for spectral parameters estimated by GWR at different spatial scales. a), b): C_a and C_b: intercept and slope of the biomass spectra, respectively; c), d): $\delta^{15}N_a$ and $\delta^{15}N_b$: intercept and slope of the $\delta^{15}N$ spectra, respectively.

Figure 1S. Relationship between the depth of the chlorophyll maximum (DCM, m) and the vertical flux of nitrate across the pycnocline by mechanical diffusion and salt fingers ($Flux[NO_3]_{tsf}$, μmol m^{-2} d^{-1}). Nitrate fluxes from Fernández-Castro *et al.* (Fernández-Castro *et al.*, 2015).

Figure 2S. Variability of a) biomass (C, mg m^{-3}) and b) $\delta^{15}N$ values (‰) with mean organism size [$\log_2$(w)]. Samples for all stations were plotted together.

Figure 3S. Distribution of (a, b) intercept (C_a, $\delta^{15}N_a$) and (c, d) slope (C_b, $\delta^{15}N_b$) of biomass and $\delta^{15}N$ plankton size spectra, respectively, e) *Trichodesmium* abundance (Tricho, log trichomes m^{-3}), (f) primary production (mg C m^{-2} d^{-1}), g) mean dust deposition (MDU, g m^{-2}), h) depth of the chlorophyll maximum (DCM, m), i) integrated chlorophyll-a concentration (Chl*a*, mg m^{-2}), j) mixed layer depth (MLD, m), k) mean squared Brunt-Väisälä frequency (N^2m, 10^{-4} s^{-2}), and l) standard deviation of the squared Brunt-Väisälä frequency (N^2sd ,10^{-4} s^{-2} measured or estimated for stations sampled during the Malaspina-2010 expedition.

689 Figure 4S. Relationship between the slope of the isotope spectrum ($\delta^{15}N_b$) and the trophic position
690 of plankton in the size fraction 2000-5000 µm (TP_{2000}). Trophic position computed as
691 $TP_{2000}=TP_{base}+(\delta^{15}N_{2000}-\delta^{15}N_{base})/\Delta^{15}N$, where TP_{base} is the trophic position of the baseline (1.5,
692 estimated as a mixture of phyto- and zooplankton in the size-fraction 40-200 µm), $\delta^{15}N_{base}$ is the
693 measured $\delta^{15}N$ in the 40-200 µm size-fraction and $\Delta^{15}N$ the average increase in $\delta^{15}N$ between
694 trophic levels (e.g. Post, 2002). The white dots represent outliers ($\delta^{15}N_b > -0.7$) and were not used in
695 the regression.

Tables

Table 1. Mean±se values of the parameters of the size spectra for biomass (C_a: intercept; C_b: slope) and $\delta^{15}N$ ($\delta^{15}N_a$: intercept; $\delta^{15}N_b$: slope) and of carbon biomass ($C_{40\text{-}200}$, mg C m^{-3}) and $\delta^{15}N$ ($\delta^{15}N_{40\text{-}200}$, ‰) for the 40-200 μm size class in the three biomass sampled. Means not significantly different are marked in the same group (ANOVA and Dunnett-C test, $P<0.05$). n: number of data.

variable	biome	mean	se	n	group
C_a	Coastal	8.840	0.166	11	a
	Westerlies	7.954	0.095	55	b
	Trades	8.961	0.071	79	a
C_b	Coastal	-0.871	0.021	11	a
	Westerlies	-0.941	0.009	55	b
	Trades	-0.884	0.006	79	a
$\delta^{15}N_a$	Coastal	10.589	0.230	11	a
	Westerlies	9.444	0.163	55	b
	Trades	10.444	0.183	79	a
$\delta^{15}N_b$	Coastal	-0.867	0.008	11	a
	Westerlies	-0.824	0.010	55	a
	Trades	-0.832	0.012	79	a
C_{40}	Coastal	1.314	0.193	11	a
	Westerlies	1.083	0.068	55	a
	Trades	1.491	0.090	79	a
$\delta^{15}N_{40}$	Coastal	5.520	0.881	11	a
	Westerlies	2.723	0.422	55	b
	Trades	5.810	0.365	79	a

709 Table 2. Mean±se values of the trophic position of the 2000-5000 µm size-class (TP_{2000}) and food
710 web parameters derived from size spectra in the three biomass sampled. NTL: number of trophic
711 levels (Zhou, 2006); PPMR: predator-to-prey mass ratio (Jennings et al., 2001); TTE: trophic
712 transfer efficiency, as % (Barnes et al., 2010). Means not significantly different are marked in the
713 same group (ANOVA and Dunnett-C test, $P<0.05$). n: number of data.
714
715

variable	biome	mean	se	n	group
TP_{2000}	Coastal	1.47	0.12	11	b
	Westerlies	1.91	0.07	55	a
	Trades	1.95	0.07	79	a
NTL	Coastal	2.81	0.07	11	a
	Westerlies	2.60	0.03	55	b
	Trades	2.76	0.02	79	a
PPMR	Coastal	696.71	199.75	11	a
	Westerlies	378.49	148.22	55	a
	Trades	723.12	203.19	79	a
TTE	Coastal	16.44	1.55	11	b
	Westerlies	24.91	1.72	55	a
	Trades	21.66	1.42	79	a, b

716
717
718

Table 3. Median, minimum (min) and maximum (max) values of GWR coefficients for spectral parameters (C_a, $\delta^{15}N_a$ and $\delta^{15}N_b$) estimated from logarithmic *Trichodesmium* abundance (Tricho, log trichomes m^{-3}), depth of chlorophyll maximum (DCM, m) and mean monthly dust deposition (g m^{-2} $month^{-1}$). All models were fit with $P<0.05$ and include a constant term. Values from models for C_b are not shown as GWR was not significant for this variable.

	constant			Tricho			DCM			MDU		
Dependent	median	min	max	median	min	max	median	min	max	median	min	max
C_a	9.162	5.842	12.391	0.001	-0.036	0.058	-0.002	-0.032	0.004	0.327	-5.685	7.134
$\delta^{15}N_a$	11.194	7.444	15.799	-0.004	-0.076	0.063	-0.002	-0.045	0.029	-2.416	-20.418	3.535
$\delta^{15}N_b$	-0.879	-1.473	-0.722	0.000	-0.003	0.004	0.000	-0.001	0.004	0.089	-0.088	0.682

Supplement

Table 1S. Parameters of the biomass-normalized biomass and $\delta^{15}N$ size-spectra determined for plankton in the 0-200 m layer of stations of the Malaspina-2010 expedition. Lines in the form $Y = a + b \log_2(w)/\Delta w$ were fitted by least squares. w: mean individual size (µg C) of organisms in each size-class; Δw: range of w for each size interval; r: correlation coefficient, se: standard error of the regression. All parameters were significant ($P<0.05$).

						biomass spectra				$\delta^{15}N$ spectra			
leg	station	date	longitude	latitude	biome	a	b	r	se	a	b	r	se
1	10	26/12/2010	-26.0016	14.5195	Trades	8.648	-0.847	-0.995	0.426	10.401	-0.804	-0.997	0.293
1	13	29/12/2010	-25.9957	7.3283	Trades	9.021	-0.874	-0.995	0.459	10.047	-0.830	-0.990	0.606
1	15	31/12/2010	-26.0169	2.4625	Trades	7.858	-0.752	-0.981	0.753	10.840	-0.830	-0.993	0.489
1	17	02/01/2011	-27.3265	-3.0306	Trades	8.877	-0.761	-0.979	0.813	10.874	-0.830	-0.993	0.506
2	35	27/01/2011	-11.8002	-28.6088	Trades	7.952	-0.844	-0.953	1.373	10.971	-0.893	-0.992	0.566
2	39	31/01/2011	0.9678	-30.8815	Trades	9.379	-0.938	-0.972	1.146	11.352	-0.829	-0.995	0.430
3	45	13/02/2011	25.5633	-35.1366	Coastal	9.100	-0.756	-0.996	0.345	11.171	-0.899	-0.991	0.622
3	46	14/02/2011	27.5456	-34.8371	Coastal	9.259	-0.953	-0.986	0.808	10.666	-0.874	-0.990	0.634
3	47	15/02/2011	31.0858	-34.4448	Coastal	8.786	-0.899	-0.991	0.606	10.597	-0.852	-0.994	0.471
3	48	16/02/2011	33.7251	-34.1728	Trades	8.529	-0.924	-0.966	1.263	10.550	-0.896	-0.987	0.752
3	49	17/02/2011	37.0018	-33.8828	Trades	8.606	-0.808	-0.992	0.532	10.702	-0.864	-0.993	0.535
3	50	18/02/2011	39.8805	-33.5322	Trades	7.522	-0.999	-0.996	0.467	10.625	-0.913	-0.993	0.548
3	51	19/02/2011	43.2477	-33.1928	Trades	8.651	-0.882	-0.986	0.773	10.626	-0.899	-0.988	0.707
3	52	23/02/2011	63.2474	-27.9776	Trades	8.826	-0.846	-0.991	0.593	10.521	-0.855	-0.999	0.233
3	53	25/02/2011	66.4931	-28.1283	Trades	9.123	-0.837	-0.990	0.595	10.225	-0.864	-0.994	0.483
3	54	26/02/2011	69.4122	-29.3618	Trades	8.768	-0.821	-0.991	0.560	10.653	-0.860	-0.995	0.443
3	55	27/02/2011	72.4499	-29.5619	Trades	8.495	-0.899	-0.971	1.130	10.651	-0.875	-0.995	0.429
3	56	28/02/2011	76.0806	-29.9046	Trades	8.243	-0.912	-0.967	1.224	11.080	-0.866	-0.993	0.530
3	57	01/03/2011	79.6065	-29.8342	Trades	8.741	-0.861	-0.986	0.743	10.889	-0.893	-0.990	0.639
3	58	02/03/2011	82.6240	-29.8106	Trades	8.614	-0.853	-0.989	0.658	11.313	-0.856	-0.995	0.456
3	59	03/03/2011	86.2619	-29.7575	Trades	8.298	-0.973	-0.979	1.027	11.508	-0.856	-0.994	0.489
3	60	04/03/2011	89.4798	-29.6831	Trades	8.762	-0.871	-0.982	0.864	11.169	-0.866	-0.990	0.638
3	61	05/03/2011	92.9838	-29.6423	Trades	8.681	-0.783	-0.994	0.443	11.076	-0.870	-0.991	0.597
3	62	06/03/2011	96.3948	-29.5818	Trades	8.931	-0.798	-0.985	0.718	11.128	-0.864	-0.992	0.564

3	63	07/03/2011	99.9978	-29.9066	Trades	8.661	-0.878	-0.984	0.816	11.443	-0.892	-0.993	0.553
3	64	08/03/2011	103.3091	-30.3329	Trades	8.463	-0.885	-0.982	0.880	10.820	-0.851	-0.991	0.578
3	65	09/03/2011	107.2080	-30.8139	Trades	8.800	-0.857	-0.984	0.785	10.294	-0.916	-0.993	0.576
3	66	10/03/2011	110.1896	-31.1453	Coastal	9.240	-0.840	-0.982	0.828	9.554	-0.871	-0.994	0.481
3	67	11/03/2011	113.4476	-31.5598	Coastal	8.529	-0.884	-0.965	1.227	10.195	-0.857	-0.984	0.786
3	68	12/03/2011	113.3935	-31.5493	Coastal	9.933	-0.836	-0.995	0.420	9.999	-0.878	-0.991	0.620
4	69	18/03/2011	120.8448	-36.6445	Coastal	8.216	-0.900	-0.950	1.515	11.232	-0.883	-0.992	0.574
4	70	19/03/2011	124.8610	-37.3508	Westerlies	8.536	-0.909	-0.981	0.927	11.327	-0.911	-0.988	0.728
4	71	20/03/2011	127.7512	-37.8550	Westerlies	9.244	-0.886	-0.986	0.757	11.692	-0.873	-0.991	0.619
4	72	21/03/2011	131.5408	-38.5484	Westerlies	8.957	-0.931	-0.983	0.880	12.015	-0.874	-0.992	0.564
4	73	22/03/2011	135.2284	-39.2225	Westerlies	9.408	-0.932	-0.990	0.668	11.912	-0.872	-0.992	0.558
4	74	23/03/2011	138.7843	-39.8431	Westerlies	9.016	-0.820	-0.981	0.835	11.969	-0.854	-0.993	0.527
4	75	24/03/2011	142.5004	-40.5312	Westerlies	8.595	-0.965	-0.988	0.765	11.915	-0.886	-0.992	0.560
4	76	25/03/2011	146.5807	-39.2681	Coastal	9.077	-0.776	-0.987	0.638	11.959	-0.888	-0.993	0.533
4	77	27/03/2011	150.4144	-38.6609	Coastal	8.207	-0.829	-0.979	0.888	10.974	-0.884	-0.991	0.613
4	78	28/03/2011	150.9914	-36.6807	Coastal	8.749	-0.979	-0.987	0.816	10.990	-0.856	-0.992	0.562
5	79	17/04/2011	176.0029	-34.0518	Trades	8.848	-0.864	-0.985	0.768	11.143	-0.868	-0.995	0.462
5	82	19/04/2011	-179.5199	-25.4835	Trades	8.915	-0.953	-0.986	0.811	9.772	-0.882	-0.990	0.648
5	83	20/04/2011	-178.2187	-23.3642	Trades	9.081	-0.892	-0.985	0.805	9.160	-0.921	-0.986	0.798
5	84	21/04/2011	-176.9193	-20.6623	Trades	9.067	-0.907	-0.996	0.392	8.698	-0.799	-0.982	0.788
5	85	22/04/2011	-175.8323	-18.5553	Trades	8.476	-0.925	-0.996	0.432	9.583	-0.895	-0.983	0.857
5	86	23/04/2011	-174.4879	-15.9029	Trades	8.556	-0.917	-0.982	0.909	11.151	-0.886	-0.991	0.599
5	87	24/04/2011	-173.3727	-13.5315	Trades	8.525	-1.023	-0.977	1.140	11.617	-0.891	-0.989	0.695
5	88	25/04/2011	-172.6531	-11.2152	Trades	8.601	-0.860	-0.978	0.948	11.995	-0.861	-0.992	0.550
5	89	26/04/2011	-172.3362	-9.4545	Trades	8.593	-0.900	-0.986	0.774	12.101	-0.861	-0.992	0.568
5	90	27/04/2011	-171.4322	-7.0484	Trades	9.987	-0.928	-0.988	0.734	11.115	-0.858	-0.992	0.566
5	91	28/04/2011	-170.7707	-5.7366	Trades	8.445	-0.812	-0.965	1.127	10.261	-0.854	-0.987	0.702
5	92	29/04/2011	-169.4625	-3.4106	Trades	9.120	-0.905	-0.988	0.730	10.176	-0.864	-0.991	0.587
5	93	30/04/2011	-168.3567	-1.3037	Trades	9.710	-0.855	-0.984	0.783	10.590	-0.842	-0.993	0.503
5	94	01/05/2011	-166.8465	1.6188	Trades	10.179	-0.889	-0.986	0.758	10.889	-0.853	-0.992	0.539
5	95	02/05/2011	-165.7639	3.7850	Trades	10.878	-0.892	-0.991	0.600	10.964	-0.850	-0.992	0.540
5	96	03/05/2011	-164.4105	6.9823	Trades	9.659	-0.825	-0.984	0.766	11.857	-0.869	-0.992	0.582
5	97	04/05/2011	-163.5270	9.2177	Trades	8.987	-0.828	-0.984	0.776	11.913	-0.849	-0.995	0.440
5	98	05/05/2011	-162.4108	11.5919	Trades	7.868	-0.835	-0.975	0.977	11.242	-0.825	-0.994	0.455
5	99	06/05/2011	-160.8179	14.9963	Trades	8.716	-0.841	-0.984	0.768	11.215	-0.867	-0.990	0.629
6	101	14/05/2011	-155.6640	21.8908	Trades	7.891	-0.923	-0.954	1.487	10.190	-0.869	-0.988	0.684
6	102	15/05/2011	-153.4199	21.5712	Trades	8.774	-0.857	-0.989	0.669	9.903	-0.870	-0.983	0.836

6	103	16/05/2011	-150.3591	21.0660	Trades	8.947	-0.848	-0.989	0.644	11.371	-0.868	-0.994	0.498
6	104	17/05/2011	-148.3402	20.8025	Trades	7.580	-0.872	-0.986	0.764	11.193	-0.862	-0.993	0.525
6	105	19/05/2011	-145.2160	20.3406	Trades	8.886	-0.808	-0.992	0.538	10.278	-0.806	-0.995	0.398
6	106	20/05/2011	-141.6154	19.8989	Trades	8.320	-0.824	-0.993	0.503	11.293	-0.859	-0.994	0.492
6	107	21/05/2011	-138.9657	19.2792	Trades	8.751	-0.840	-0.990	0.626	11.496	-0.873	-0.992	0.550
6	108	22/05/2011	-136.1774	18.6483	Trades	9.273	-0.908	-0.995	0.448	11.678	-0.849	-0.991	0.600
6	109	23/05/2011	-133.2623	18.0538	Trades	9.282	-0.866	-0.984	0.791	11.381	-0.867	-0.992	0.578
6	110	24/05/2011	-130.5909	17.4013	Trades	9.592	-0.951	-0.988	0.752	11.418	-0.862	-0.993	0.507
6	111	25/05/2011	-127.5755	16.6239	Trades	9.384	-0.887	-0.977	0.988	11.692	-0.860	-0.991	0.604
6	112	26/05/2011	-124.5040	15.9132	Trades	8.919	-0.781	-0.979	0.832	11.780	-0.847	-0.994	0.464
6	113	27/05/2011	-121.9954	15.3108	Trades	9.244	-0.880	-0.976	1.003	11.750	-0.868	-0.992	0.567
6	115	28/05/2011	-115.7725	13.7653	Trades	9.673	-0.932	-0.971	1.168	11.736	-0.857	-0.994	0.465
6	116	29/05/2011	-113.2701	13.1952	Trades	9.160	-0.952	-0.973	1.158	11.398	-0.838	-0.988	0.659
6	117	30/05/2011	-110.3917	12.4943	Trades	9.301	-0.908	-0.985	0.809	11.633	-0.865	-0.993	0.513
6	118	31/05/2011	-108.0495	11.9936	Trades	9.401	-0.949	-0.974	1.136	11.736	-0.857	-0.992	0.543
6	119	01/06/2011	-105.0116	11.3552	Trades	9.233	-0.861	-0.980	0.901	11.599	-0.857	-0.994	0.465
6	120	02/06/2011	-102.4479	10.7564	Trades	9.956	-0.872	-0.981	0.870	11.616	-0.874	-0.991	0.590
6	121	03/06/2011	-99.2499	10.0847	Trades	9.344	-0.906	-0.984	0.847	11.748	-0.854	-0.993	0.510
6	122	04/06/2011	-96.3360	9.4393	Trades	9.951	-0.821	-0.992	0.531	11.726	-0.863	-0.994	0.484
6	123	05/06/2011	-93.1477	8.7615	Trades	9.963	-0.810	-0.955	1.289	11.067	-0.864	-0.993	0.528
6	124	06/06/2011	-90.3620	8.1413	Trades	9.415	-0.936	-0.968	1.230	10.769	-0.838	-0.992	0.556
6	125	07/06/2011	-87.9549	7.2239	Trades	10.591	-0.887	-0.978	0.976	10.694	-0.852	-0.990	0.611
6	126	08/06/2011	-84.7942	5.9111	Trades	9.030	-0.888	-0.984	0.821	11.304	-0.849	-0.994	0.481
7	129	22/06/2011	-69.2892	15.0732	Trades	9.560	-0.905	-0.969	1.183	7.679	-0.629	-0.983	0.601
7	130	23/06/2011	-67.0695	15.5763	Trades	10.316	-0.962	-0.958	1.474	9.002	-0.910	-0.975	1.067
7	131	25/06/2011	-59.8288	17.4276	Trades	8.522	-0.895	-0.990	0.637	9.125	-0.823	-0.988	0.663
7	132	26/06/2011	-57.8094	18.0651	Trades	9.067	-0.913	-0.985	0.807	5.091	-0.404	-0.600	2.749
7	133	27/06/2011	-55.1573	19.0153	Trades	8.855	-0.914	-0.983	0.868	5.977	-0.597	-0.959	0.906
7	134	28/06/2011	-52.6289	20.0110	Trades	9.137	-0.928	-0.987	0.774	3.766	-0.237	-0.847	0.758
7	135	29/06/2011	-50.1433	20.8033	Trades	8.459	-1.001	-0.991	0.708	7.210	-0.738	-0.988	0.578
7	136	30/06/2011	-47.7887	21.7383	Trades	8.809	-0.976	-0.979	1.028	6.821	-0.776	-0.783	3.148
7	137	01/07/2011	-44.5286	22.8634	Trades	8.803	-0.966	-0.982	0.948	6.207	-0.463	-0.990	0.343
7	138	02/07/2011	-41.9070	23.7336	Trades	8.835	-0.975	-0.991	0.684	8.202	-0.797	-0.966	1.083
7	139	03/07/2011	-38.7107	24.8569	Trades	9.015	-0.892	-0.989	0.667	8.371	-0.773	-0.988	0.618
7	140	04/07/2011	-35.2705	26.1084	Westerlies	8.413	-0.990	-0.977	1.100	8.924	-0.815	-0.992	0.520
7	141	05/07/2011	-32.8858	26.9174	Westerlies	8.511	-0.897	-0.994	0.515	9.459	-0.808	-0.989	0.624
7	142	06/07/2011	-29.6718	27.9803	Westerlies	8.224	-0.947	-0.987	0.783	9.737	-0.873	-0.993	0.536

7	143	07/07/2011	-26.9515	28.8747	Westerlies	8.375	-0.877	-0.992	0.583	9.758	-0.868	-0.995	0.457
7	144	08/07/2011	-23.6907	29.9667	Westerlies	9.032	-0.940	-0.985	0.836	10.052	-0.839	-0.994	0.470
7	145	09/07/2011	-20.6366	30.9602	Westerlies	9.128	-0.960	-0.985	0.846	9.980	-0.823	-0.992	0.518
8	001	28/01/2011	-13.3418	27.7750	Westerlies	10.346	-0.749	-0.990	0.552	10.549	-0.829	-0.987	0.683
8	012	29/01/2011	-15.3478	27.1285	Westerlies	8.298	-0.891	-0.992	0.573	9.893	-0.855	-0.989	0.643
8	016	30/01/2011	-16.7797	26.6630	Westerlies	7.898	-0.905	-0.998	0.295	9.845	-0.862	-0.986	0.754
8	020	31/01/2011	-18.2703	26.1837	Westerlies	7.675	-0.849	-0.979	0.903	10.572	-0.877	-0.990	0.650
8	024	01/02/2011	-20.0092	25.6257	Westerlies	7.336	-0.785	-0.994	0.430	10.342	-0.868	-0.987	0.728
8	027	02/02/2011	-21.4565	25.1563	Westerlies	7.730	-0.955	-0.987	0.794	9.954	-0.846	-0.993	0.518
8	030	03/02/2011	-22.9763	24.6612	Westerlies	7.821	-0.916	-0.998	0.257	10.275	-0.827	-0.992	0.534
8	033	04/02/2011	-24.7080	24.5012	Westerlies	7.943	-0.971	-0.994	0.540	10.161	-0.860	-0.983	0.827
8	037	05/02/2011	-27.1497	24.5012	Westerlies	7.214	-0.807	-0.990	0.573	9.523	-0.871	-0.992	0.563
8	039	06/02/2011	-28.3718	24.5010	Westerlies	7.614	-0.892	-0.993	0.552	9.166	-0.837	-0.993	0.520
8	040	07/02/2011	-28.9843	24.4990	Westerlies	7.179	-0.963	-0.991	0.648	9.302	-0.827	-0.991	0.561
8	043	08/02/2011	-30.8183	24.4992	Westerlies	7.167	-0.928	-0.982	0.906	9.537	-0.826	-0.992	0.547
8	045	09/02/2011	-32.0403	24.5010	Westerlies	7.621	-0.936	-0.996	0.420	9.113	-0.946	-0.991	0.667
8	048	10/02/2011	-33.8727	24.5008	Westerlies	6.927	-0.890	-0.986	0.755	9.311	-0.739	-0.992	0.482
8	052	11/02/2011	-34.7195	24.4998	Westerlies	7.459	-1.004	-0.995	0.507	8.613	-0.835	-0.984	0.774
8	055	12/02/2011	-37.1078	24.5017	Westerlies	7.542	-0.901	-0.994	0.494	8.392	-0.957	-0.982	0.941
8	059	13/02/2011	-38.9537	24.4998	Westerlies	7.670	-0.963	-0.999	0.264	8.942	-0.843	-0.996	0.366
8	061	14/02/2011	-39.8760	24.5022	Westerlies	7.480	-0.768	-0.995	0.388	8.218	-0.686	-0.995	0.336
8	064	15/02/2011	-41.2633	24.4998	Westerlies	7.567	-0.994	-0.995	0.494	8.746	-0.784	-0.983	0.748
8	068	16/02/2011	-43.1097	24.5002	Westerlies	7.578	-1.000	-0.998	0.339	8.838	-0.788	-0.994	0.458
8	071	17/02/2011	-44.4953	24.4998	Westerlies	7.388	-0.883	-0.994	0.489	8.390	-0.872	-0.953	1.410
8	075	18/02/2011	-46.3437	24.5000	Westerlies	7.932	-1.023	-0.996	0.457	8.200	-0.745	-0.981	0.761
8	078	19/02/2011	-47.7278	24.5007	Westerlies	7.666	-0.891	-0.993	0.551	7.924	-0.820	-0.979	0.866
8	082	20/02/2011	-49.5755	24.5000	Westerlies	7.103	-1.075	-0.992	0.709	8.676	-0.791	-0.988	0.632
8	085	21/02/2011	-50.9612	24.5002	Westerlies	7.647	-0.929	-0.985	0.821	8.209	-0.721	-0.964	1.013
8	088	22/02/2011	-52.3467	24.5000	Westerlies	7.465	-0.991	-0.998	0.310	8.061	-0.938	-0.944	1.678
8	091	23/02/2011	-54.0342	24.4865	Westerlies	7.224	-0.963	-0.997	0.377	7.622	-0.602	-0.978	0.660
8	094	24/02/2011	-55.8743	24.5005	Westerlies	7.109	-0.970	-0.993	0.587	7.297	-0.982	-0.829	3.384
8	097	25/02/2011	-57.7157	24.5008	Westerlies	7.164	-0.971	-0.994	0.528	6.013	-0.561	-0.582	4.002
8	100	26/02/2011	-59.5530	24.5000	Westerlies	7.556	-1.045	-0.995	0.510	8.878	-0.728	-0.978	0.787
8	104	27/02/2011	-62.0047	24.5012	Westerlies	7.079	-0.984	-0.988	0.772	8.200	-0.792	-0.968	1.052
8	107	28/02/2011	-63.8430	24.5015	Westerlies	7.165	-0.991	-0.993	0.611	8.391	-0.703	-0.997	0.282
8	110	01/03/2011	-65.6820	24.5007	Westerlies	8.001	-0.984	-0.993	0.612	8.770	-0.804	-0.987	0.658
8	113	02/03/2011	-67.5202	24.4997	Westerlies	7.807	-1.025	-0.996	0.461	8.773	-0.734	-0.994	0.423

8	116	03/03/2011	-69.1327	24.5007	Westerlies	7.992	-1.017	-0.998	0.287	8.934	-0.817	-0.986	0.703
8	120	05/03/2011	-70.3220	26.2038	Westerlies	7.990	-1.031	-0.995	0.525	9.364	-0.786	-0.991	0.545
8	125	06/03/2011	-72.2647	26.2032	Westerlies	8.083	-1.013	-1.000	0.047	9.738	-0.839	-0.987	0.707
8	128	07/03/2011	-73.4317	26.2035	Westerlies	7.862	-1.026	-0.997	0.387	9.297	-0.789	-0.986	0.689
8	133	08/03/2011	-75.1557	26.2038	Westerlies	8.165	-0.936	-0.998	0.280	9.412	-0.904	-0.980	0.936
8	137	09/03/2011	-75.8622	26.2042	Westerlies	7.957	-0.993	-0.998	0.297	9.855	-0.799	-0.995	0.411
8	143	10/03/2011	-76.6218	26.2037	Westerlies	8.192	-0.961	-0.999	0.258	9.899	-0.856	-0.992	0.560
8	149	11/03/2011	-76.9525	26.2030	Westerlies	8.656	-0.961	-0.995	0.496	9.928	-0.797	-0.995	0.426
8	157	13/03/2011	-79.3063	27.0003	Westerlies	8.753	-0.962	-0.993	0.590	9.781	-0.830	-0.994	0.447
8	161	13/03/2011	-79.5658	27.0012	Coastal	8.138	-0.926	-0.997	0.349	9.784	-0.813	-0.996	0.385

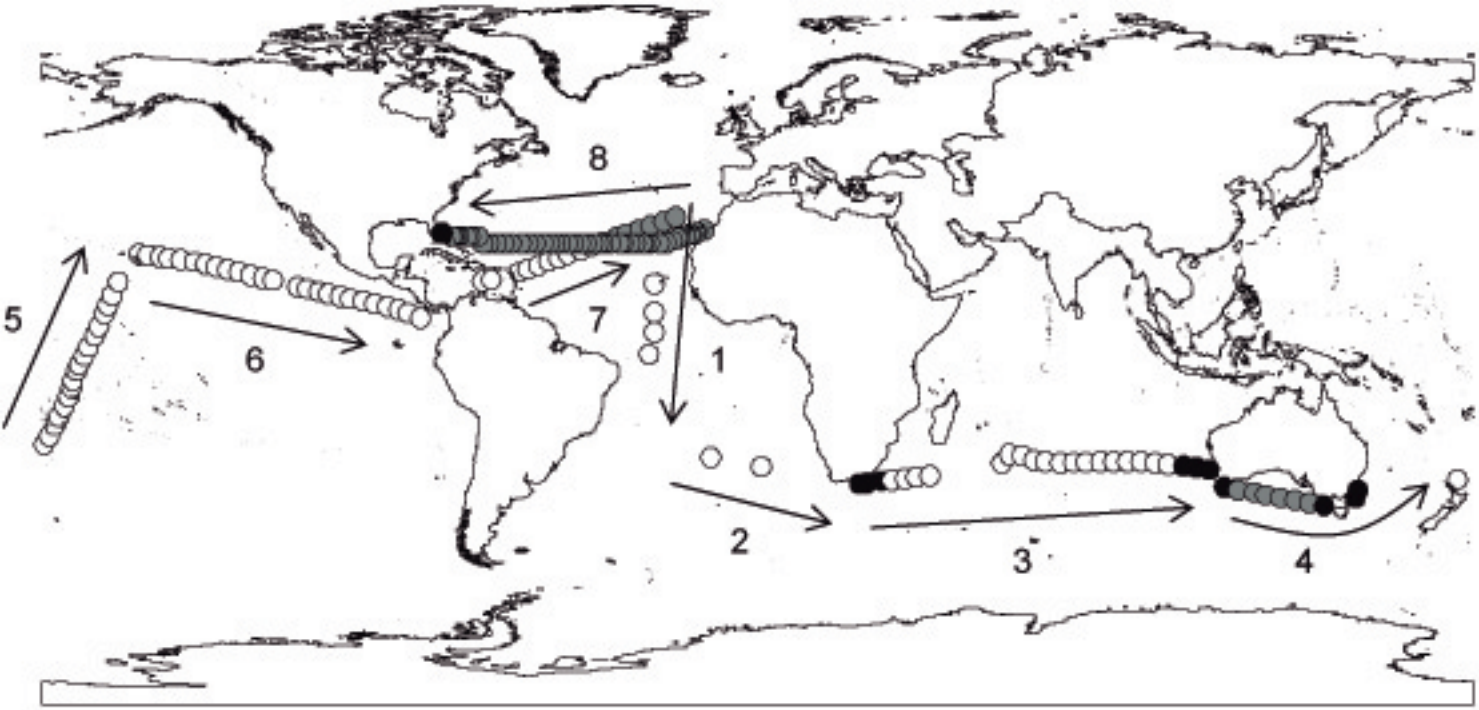
8
5
6
7
1
2
3
4

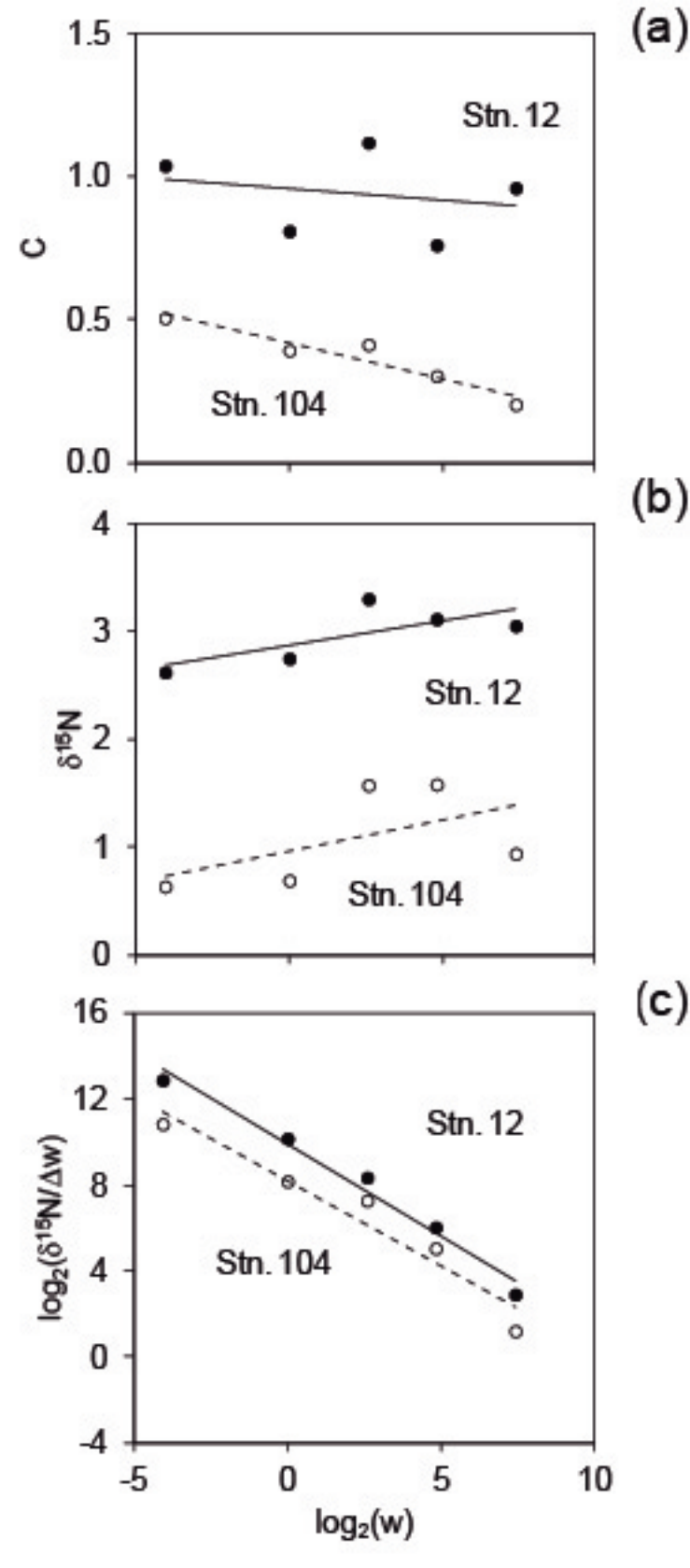
(a)
1.5
1.0
0.5
0.0
C
Stn. 12
Stn. 104
(b)
4
3
2
1
0
δ15N
Stn. 12
Stn. 104
(c)
16
12
8
4
0
-4
log2(δ15N/Δw)
Stn. 12
Stn. 104
-5
0
5
10
log2(w)

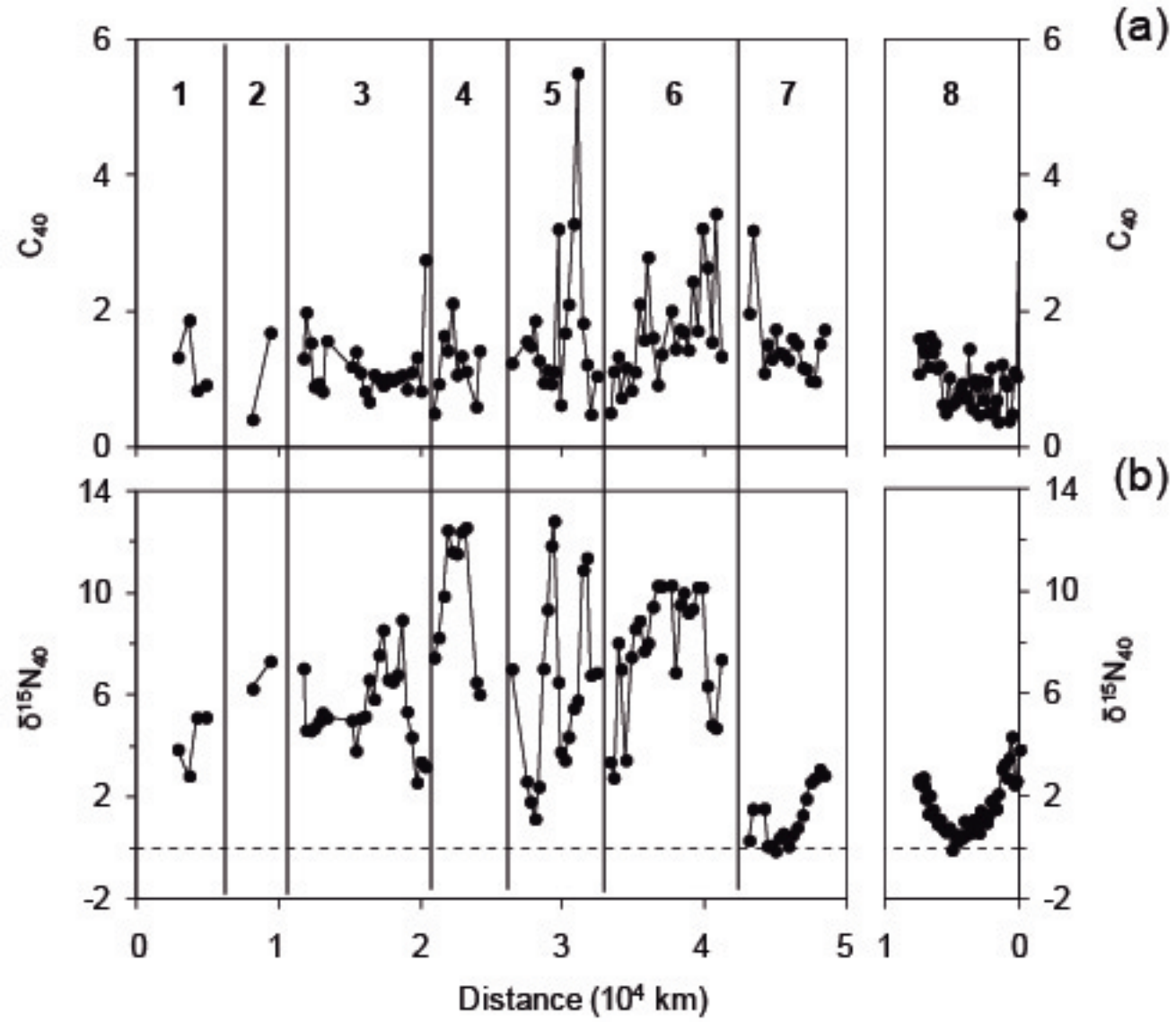
(a)
(b)
1
2
3
4
5
6
7
8
C_{40}
$\delta^{15}N_{40}$
Distance (10^4 km)

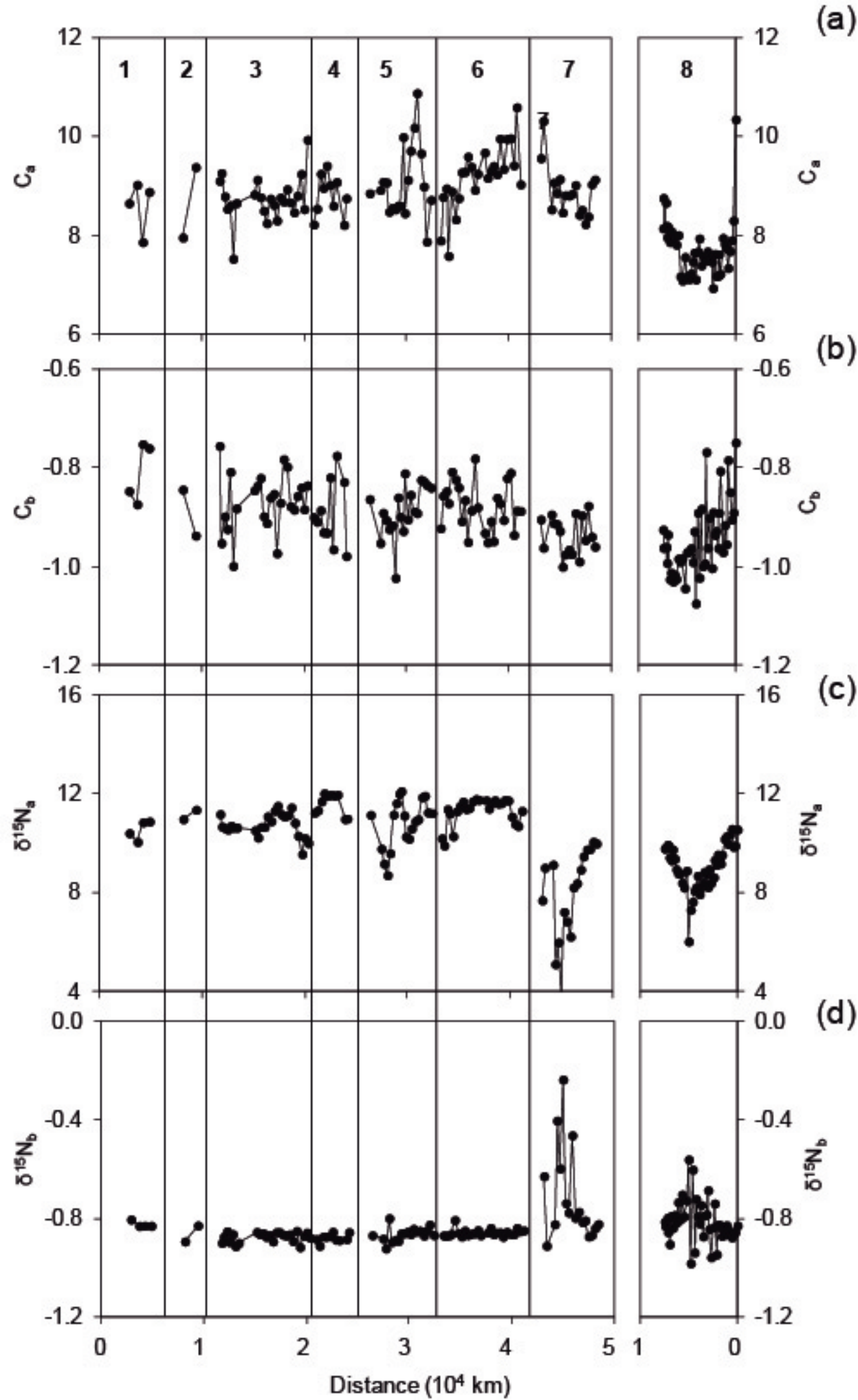
(a)
(b)
(c)
(d)
1
2
3
4
5
6
7
8
C_a
C_b
$\delta^{15}N_a$
$\delta^{15}N_b$
Distance (10^4 km)

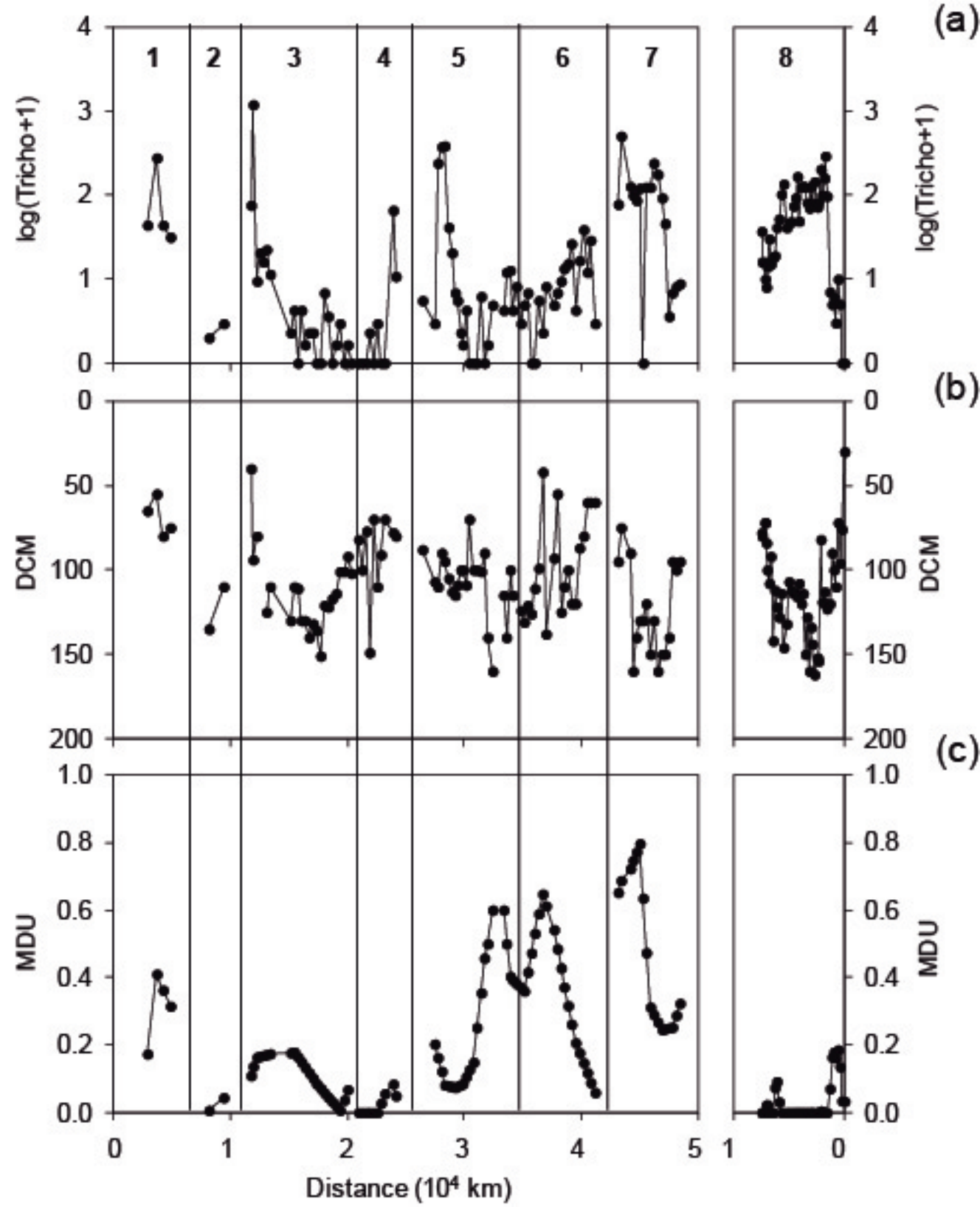
(a)
(b)
(c)
1
2
3
4
5
6
7
8
log(Tricho+1)
DCM
MDU
Distance (10^4 km)

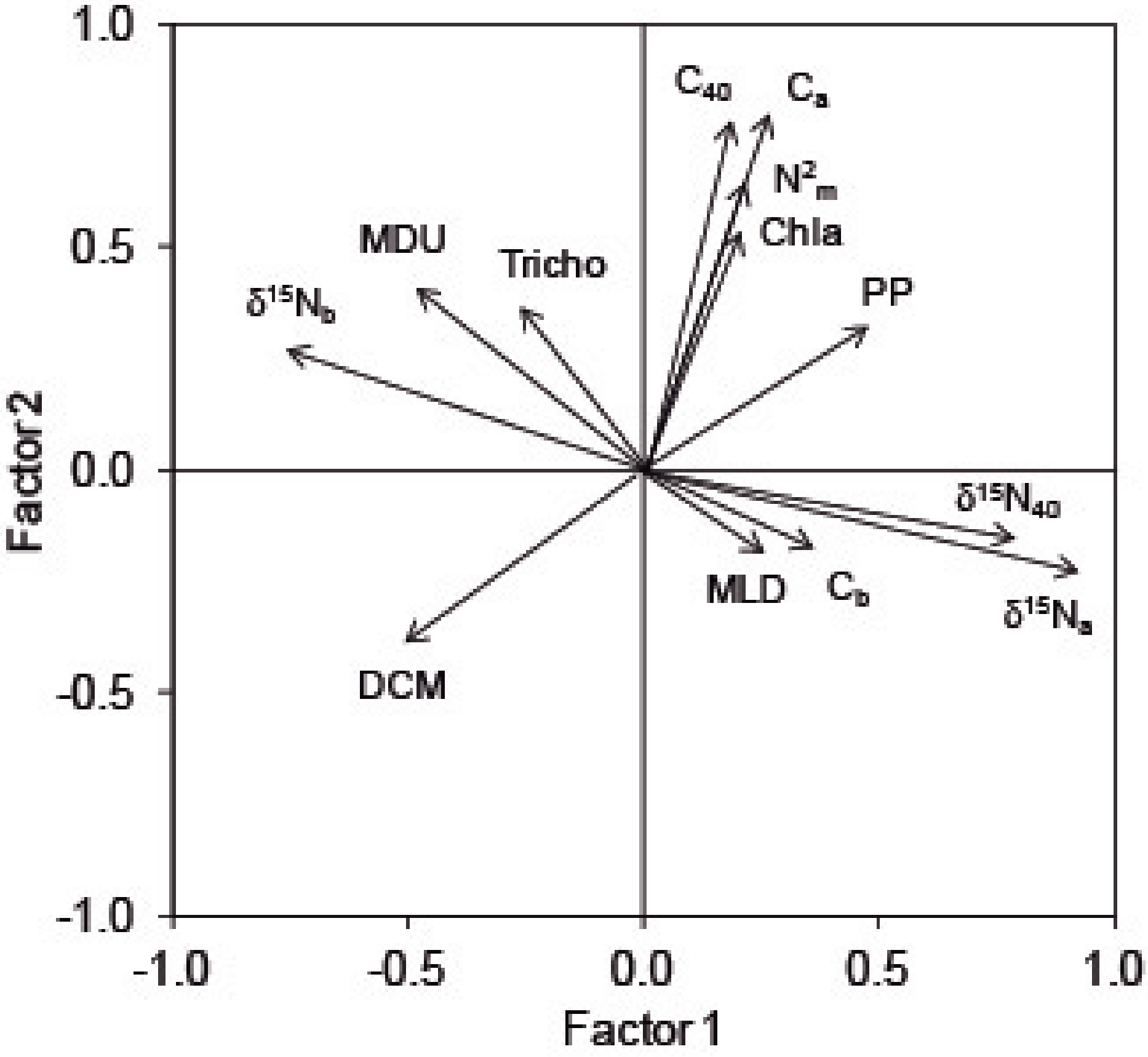
1.0
0.5
0.0
-0.5
-1.0
Factor 2
-1.0
-0.5
0.0
0.5
1.0
Factor 1
C40
Cs
N2m
Chla
MDU
Tricho
δ15Nb
PP
δ15N40
MLD
Cb
δ15Ns
DCM

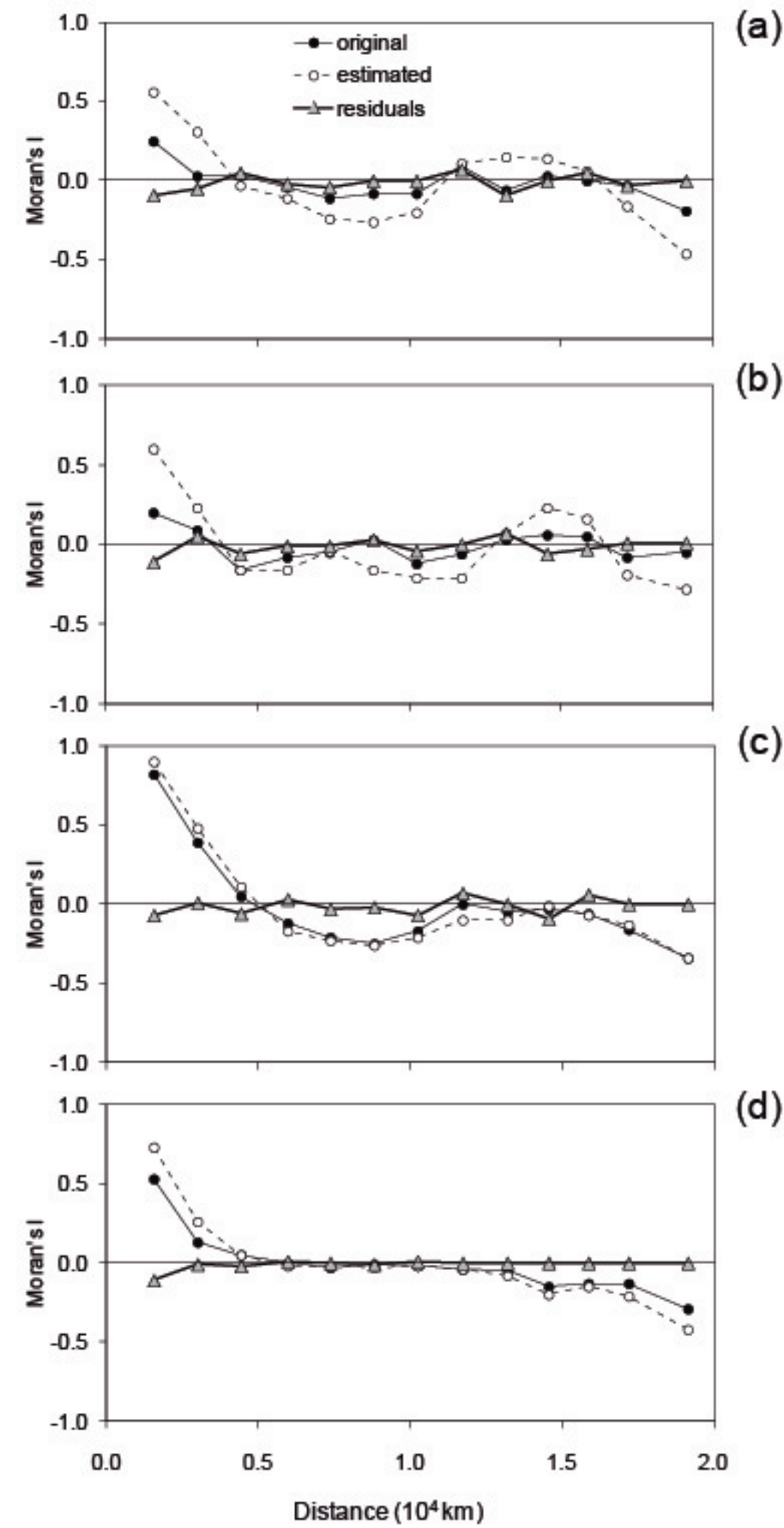
(a)
original
estimated
residuals
Moran's I
1.0
0.5
0.0
-0.5
-1.0
(b)
Moran's I
1.0
0.5
0.0
-0.5
-1.0
(c)
Moran's I
1.0
0.5
0.0
-0.5
-1.0
(d)
Moran's I
1.0
0.5
0.0
-0.5
-1.0
0.0
0.5
1.0
1.5
2.0
Distance (10^4 km)

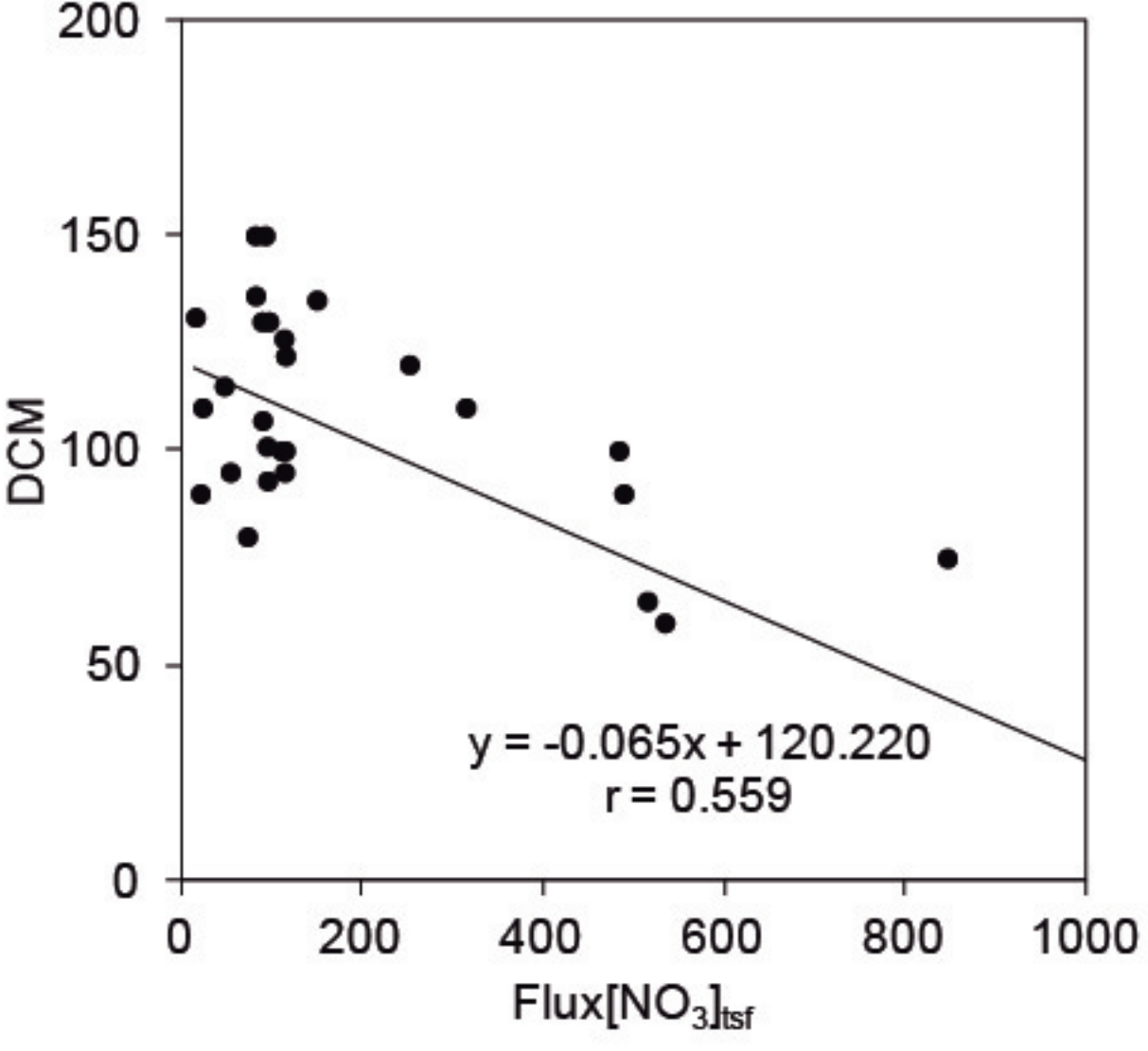
200
150
100
50
0
DCM
0
200
400
600
800
1000
Flux[NO3]tsf
y = -0.065x + 120.220
r = 0.559

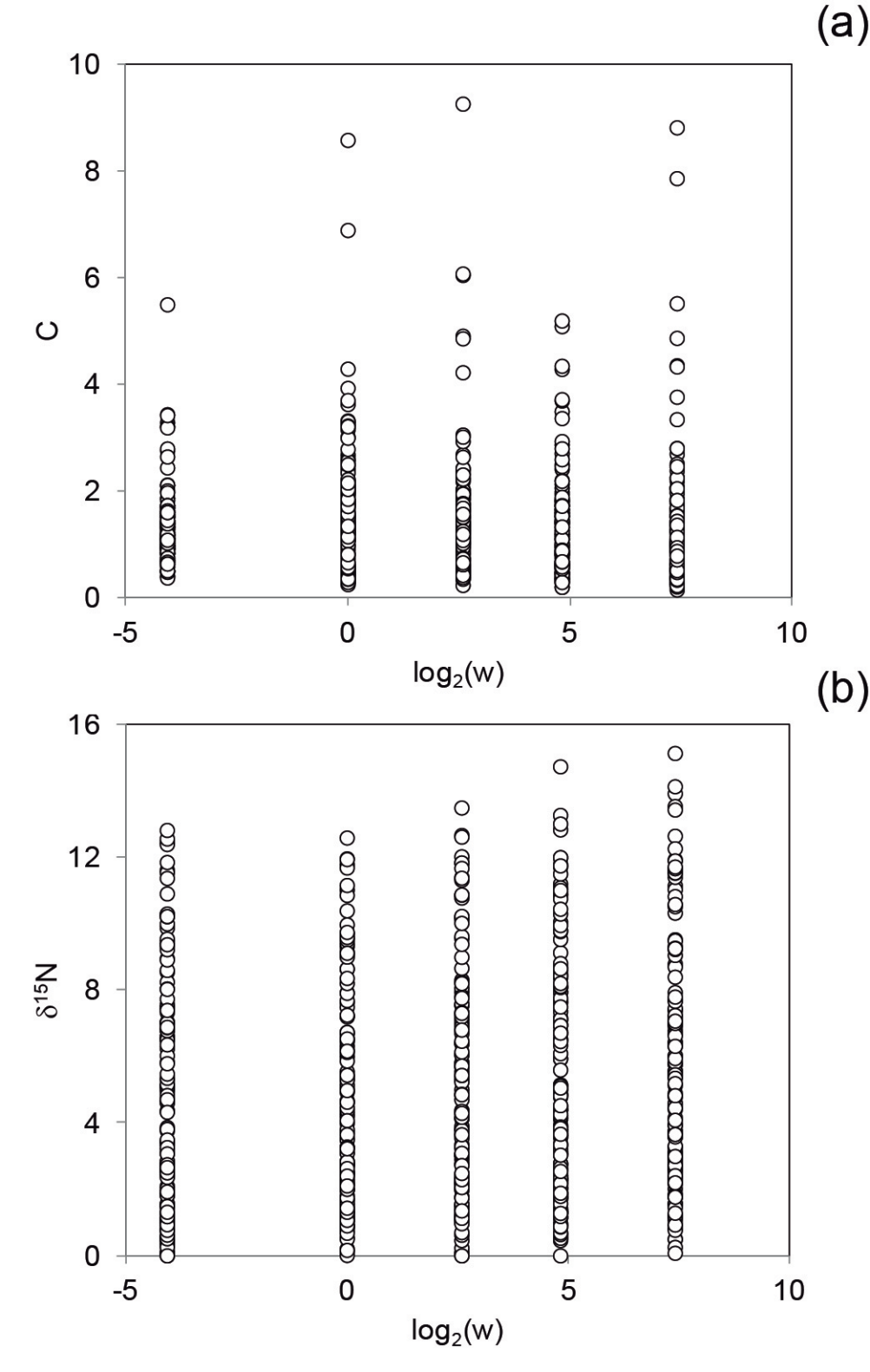
(a)
10
8
6
4
2
0
C
-5
0
5
10
log2(w)
(b)
16
12
8
4
0
δ15N
-5
0
5
10
log2(w)

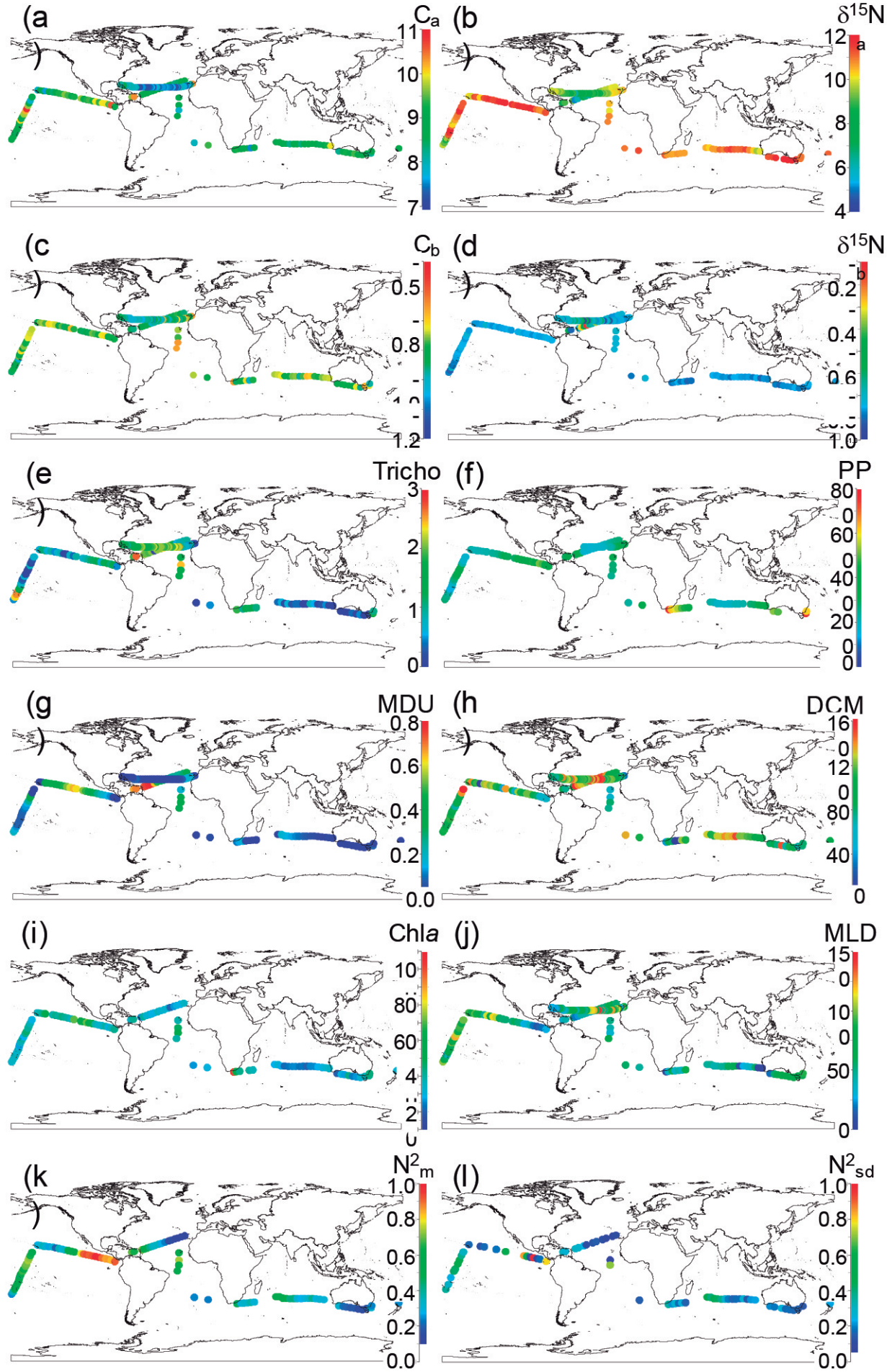
(a)
C_a
11
10
9
8
7
(b)
$\delta^{15}N$
a
12
10
8
6
4
(c)
C_b
0.5
0.8
1.2
(d)
$\delta^{15}N$
b
0.2
0.4
0.6
1.0
(e)
Tricho
3
2
1
0
(f)
PP
80
60
40
20
0
(g)
MDU
0.8
0.6
0.4
0.2
0.0
(h)
DCM
16
12
80
40
0
(i)
Chla
10
80
60
4
2
0
(j)
MLD
15
10
50
0
(k)
N^2_m
1.0
0.8
0.6
0.4
0.2
0.0
(l)
N^2_{sd}
1.0
0.8
0.6
0.4
0.2
0.0

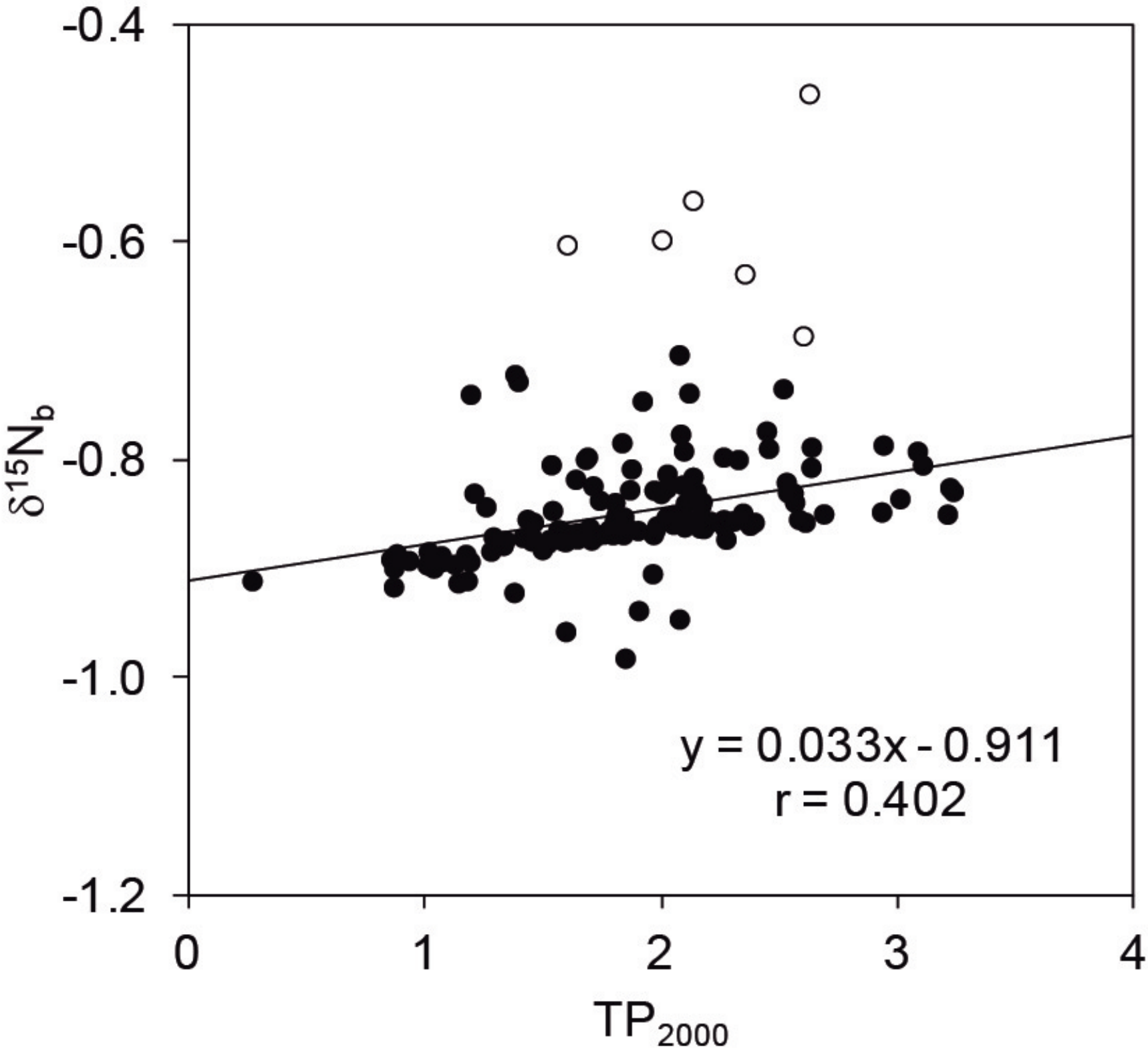
-0.4
-0.6
-0.8
-1.0
-1.2
δ15Nb
0
1
2
3
4
TP2000
y = 0.033x - 0.911
r = 0.402